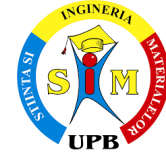**UNIVERSITY POLITEHNICA OF BUCHAREST**

Materials Science and Engineering Doctoral School

313 Splaiul Independenței, District 6, Bucharest, Zip code 060042

Phone/fax: 021 402 9624; http://www.sdsim.upb.ro

PhD Thesis Summary

Studies and research on improving the osseointegration properties of titanium through electrochemical techniques

PhD candidate: Ionuț-Cornel Ionescu

PhD Supervisor: Prof.dr.eng Mihai Ovidiu Cojocaru

DOCTORAL COMMITTEE

President	Prof.dr.habil.eng. **Florin Miculescu**	from	University Politehnica of Bucharest
PhD Supervisor	Prof.dr.eng. **Mihai Ovidiu Cojocaru**	from	University Politehnica of Bucharest
Referee	Conf.dr. **Lucian Toma Ciocan**	from	University of Medicine and Pharmacy "Carol Davila" Bucharest
Referee	Conf.dr.eng. **Bogdan Istrate**	from	”Gheorghe Asachi” Technical University of Iași
Referee	Conf.dr.eng. **Cosmin Mihai Cotruț**	from	University Politehnica of Bucharest

Bucharest
2022

Table of contents

Abstract

Currently, the biomaterials performances are conventionally improved by modifying the surface characteristics in terms of morphology/topography and/or by using functional coatings. This major necessity to modify the implants surface derives from the desire to improve the osseointegration capacity of biomaterials, to reduce the bacterial adhesion and inflammatory response.

The main objective of this PhD/doctoral thesis consists in the development of new surfaces with improved properties and characteristics in terms of electrochemical behavior, bioactivity, biocompatibility and antibacterial efficiency, by modifying the surface of Ti-based metallic biomaterials through electrochemical techniques in order to obtain a nanostructured surface made of a titanium dioxide nanotubes (TiO_2 NT), and subsequently coated with a bioactive ceramic layer of undoped hydroxyapatite (H) and doped with biocompatible elements such as Mg (H-Mg) or Zn (H-Zn).

The nanostructured surface with titanium dioxide nanotubes (TiO_2 NT) obtained by anodic oxidation of pure Ti, in an electrolyte with a concentration of 0.5 wt.% HF and applying a potential of 20V, for 30 minutes has led to a diameter of the NT of ~70 nm , a good wettability and better corrosion resistance, compared to pure Ti. Subsequently, the TiO_2 NT nanostructured surface, was biofunctionalized with undoped HAp based coatings and doped with Mg or Zn in different concentrations, using the electrochemical pulsed galvanostatic deposition technique. According to the obtained results in terms of adhesion and layer thickness, the samples with higher concentration of the doping element were eliminated, as they showed poorer adhesion to the nanostructured surface and notable variations of the layer thicknesses, properties that can strongly influence the further test results.

The *in vitro* assays have highlighted that addition of Mg or Zn in the HAp structure can adjust the behavior of the HAp based coatings in terms of electrochemical behavior, but can also be used to enhance the bioactivity, the osteoblast cell interaction and to offer antibacterial efficiency, depending on the type of doping element. According to the obtained results the most efficient HAp based coating was found to be the one with Zn as it presents most of the properties necessary for a proper behavior in the human body.

In conclusion it can be said that the osseointegration properties of Ti based implantable devices can be enhanced by surface modification through electrochemical means, namely anodic oxidation and electrochemical deposition in pulsed galvanostatic mode, which can also be applied on complex geometrical shapes.

Keywords: biofunctionalization, titanium dioxide nanotubes, hydroxyapatite, doping, magnesium, zinc.

Introduction

The global requirement for the usage and development of biomaterials more efficient and safer is growing considerably, being in close correlation with the annual growth rate of the world population, the increment of the elderly people and the functional demands required by younger population. Due to their characteristics such as good corrosion resistance in aggressive environments, good resistance to mechanical stress and proper biocompatibility, titanium and its alloys are considered to be one of the most important biomaterials used to date.

Titanium-based implants are very stable after implantation in the human body, this being the main reason why they are known as bioinert materials. The clinical goal and the most critical factor in the long-term success of an orthopedic or dental implant is to achieve osseointegration, by establishing a strong structural and functional bond at the biomaterial-tissue interface. Thus, the success of an implant is not only governed by the material from which it is made, but also by its surface properties (surface chemistry, topography, morphology, structure, etc.), these being critical factors in the interaction with the human tissues.

Currently, the performances of biomaterials are conventionally improved by modifying the surface characteristics in terms of morphology/topography and/or by functional coatings. This major need to modify the surface of implants derives from the desire to improve the osseointegration capacity of biomaterials, to reduce the bacterial adhesion and the inflammatory response.

Thus, this combination of properties that Ti and its alloys present, along with the wide possibilities of surface modification and biofunctionalization, make these materials suitable to be successfully used in medical applications.

The main objective of this doctoral thesis "*Studies and researches regarding the improvement of the osseointegration properties of titanium with the help of electrochemical techniques*" consists in the development of new surfaces with improved properties and characteristics, by modifying the surface of Ti based metallic biomaterials through electrochemical techniques in order to obtain a nanostructured surfaces based on titanium dioxide (TiO_2) in the form of nanotubes (NT) and coating it with a hydroxyapatite bioactive ceramic doped with biocompatible elements such as Mg or Zn.

The doctoral thesis is structured in 6 chapters, along with an introduction and conclusions of the obtained results, as well as a bibliography consisting in 246 bibliographic references.

The first two chapters include a synthesis of the studies published in the scientific literature, regarding the topic addressed in the present doctoral thesis.

1st Chapter presents a literature study which addresses the general aspects of the biomaterials used in dentistry to manufacture dental implants, with a special focused on titanium and its alloys, which are the main materials used to obtain implantable devices, as well as hydroxyapatite based ceramic biomaterials. Moreover, in this chapter are presented the fields in which these materials are used along with their specific properties and applicability.

The *2nd chapter* presents a classification of the surface biofunctionalization techniques for metallic materials by using the mechanical, physical, chemical, and electrochemical techniques, as well as through the usage of hydroxyapatite-based coatings, by emphasizing the electrochemical techniques, namely the anodic oxidation and electrochemical depositions, respectively, these being the techniques used in this doctoral thesis.

The *3rd chapter* presents the objectives of the doctoral thesis, the materials used, and the experimental research strategy carried out. The characterization techniques used in this doctoral thesis aimed a detailed physico-chemical investigation by using the scanning electron microscopy (SEM), energy dispersive X-ray spectrometry (EDS), X-ray diffraction (XRD), Fourier transform infrared spectrometry (FTIR), contact profilometry, "adhesive tape" test and scratch test, and surface energy.

A particularly important characteristic of these biomaterials is their behavior in mediums which mimic the human environment, thus, a special attention was given to testing, by evaluating the electrochemical behavior in simulated body fluid (SBF) and Fusayama Meyer artificial saliva, as well as bioactivity tests by immersion, emphasizing the capacity of biomineralization in SBF but also the biodegradation in phosphate buffer solution (PBS).

The biological compatibility was demonstrated by performing *in vitro* cell viability assay using the tetrazolium salt assay (MTT assay) to quantify the cell viability. Cell tests were performed using bone cell cultures, specifically MG63 osteoblast cells from the human osteosarcoma line.

Another important aspect addressed in the present doctoral thesis consisted in testing the bacterial efficiency of the developed surfaces. The antibacterial tests were performed on bacterial strains of *Escherichia coli – E.coli* (ATCC 25922).

Chapter 4 presents the preliminary results regarding the obtaining and characterization of the nanostructured surfaces with titanium dioxide nanotubes (NT) by using the anodic oxidation technique, as well as the electrochemical depositions of the hydroxyapatite-based coatings undoped and doped with Mg in different concentrations on a Ti alloy substrate by using the pulsed galvanostatic technique.

Chapter 5 presents the experimental results regarding the obtaining and characterization of the nanostructured surface with titanium dioxide nanotubes (NT) selected from ***chapter 4*** uncoated and coated with layers undoped hydroxyapatite (H) and doped with Mg (H-Mg) or Zn (H-Zn) in different concentrations, with the aim to evaluate the influence of the doping elements on the physico-chemical characteristics of hydroxyapatite. Based on the obtained results in this chapter, the coatings to be further tested were selected.

Thus, ***chapter 6*** presents the results obtained after testing the nanostructured surfaces with titanium dioxide nanotubes uncoated and coated with hydroxyapatite-based layers undoped and doped with Mg or Zn in optimal concentrations, in terms of electrochemical behavior, bioactivity, biocompatibility and the antibacterial efficiency.

The final chapter, entitled ***Conclusions***, summarizes the main results obtained during the elaboration of the doctoral thesis, highlighting at the same time the original contributions of the author, but also the future research directions, since the problems addressed remains open for further extensive analysis and, as the case may be, more thorough.

Part I

Chapter 1. Biomaterials used in dental medicine for dental implants manufacturing

Currently, the biomaterials are seen as indispensable in improving and extending the quality of human life, being able to be individually used or as a component of a more complex system, aiming to fulfill the functions for which it was designed [4,5]. Figure 1.1 shows a schematic illustration of the biomaterial's classification according to their chemical nature and interaction with the human body.
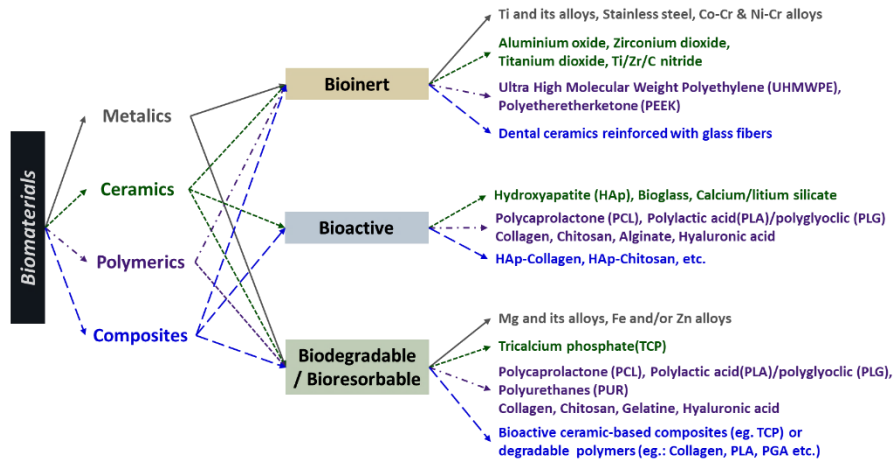
Figure 1.1. Biomaterial's classification according to their chemical nature and interaction with the human body

It is estimated that dental implants have a success rate of 90% after 10 - 15 years post-implantation. However, between 5% and 11% of the dental implants do not show proper osseointegration into the maxillofacial hard tissues. Failure of long-term dental implant stability can be due to biological (20% of them are due to peri-implantitis, microbial plaque formation or bacterial infections [82]) and mechanical (osteopenia [83]) causes. The scientific community is making considerable efforts to find the optimum, easy-to-apply, feasible and effective solutions to improve the osseointegration capacity of Ti-based implants, but also to reduce or even to eliminate the implant related infections by identifying agents, elements, and materials with antibacterial efficiency. In order to achieve this, various preparation and/or processing advanced techniques are applied, followed by appropriate surface coatings and modifications.

Chapter 2. Titanium biofunctionalization techniques

The metallic implants have been widely used to replace the damaged human bone for more than 40 years and since then has remained the most widely used. However, it is well known that metallic biomaterials do not have a bioactive character which is necessary for the implantable material to form a biological bond with adjacent tissues, and to overcome the insufficient adhesion, the surface of the metallic implants can be biofunctionalized, either by mechanical and chemical methods or with bioactive and durable coatings [85]. The most important aspect and on which the success of an implant largely depends, is the condition of the implant surface.

Figure 2.1 shows the main biofunctionalization methods used for titanium. Surface treatments or modification methods can improve the biological characteristics of implants by adding materials with specific properties, changing the composition, or removing unwanted material from the implant surface.

	TITANIUM BIOFUNCTIONALIZATION METHODS	
Methods	(A) **Surface modification methods**	(B) **HAp coatings deposition technique**
Mechanical	▪ Grinding, polishing ▪ Air-born particle abrasion with Al_2O_3, SiC, TiO_2	▪ —
Physical	▪ Plasma treatment ▪ Laser ablation ▪ Ionic implantation	▪ Physical vapor deposition (PVD) ▪ Magnetron sputtering ▪ Plasma spraying ▪ Thermal spraying ▪ Pulsed laser deposition ▪ Microwave irradiation / treatment ▪ High temperature oxidation ▪ Ion/electron beam assisted deposition
Chemical	▪ H_2O_2 treatment ▪ Alkaline treatment (NaOH, KOH) ▪ Acidic treatment (HF)	▪ Chemical vapor deposition (CVD) ▪ Biomimetic method ▪ Sol-gel method ▪ Hydrothermal method
Electrochemical	▪ Anodic oxidation ▪ Electrochemical polishing	▪ Electrochemical deposition ▪ Electrophoretic deposition ▪ Plasma electrolytic oxidation

Figure 2.1. *Classification of the main titanium biofunctionalization methods*

2.3 Development of the nanostructured surface by anodic oxidation

Anodic oxidation is a versatile technique, able to modify the properties of the obtained oxide by changing and/or adjusting the electrochemical parameters (applied potential, electrolyte composition and concentration, anodization time, process temperature, electrolyte stirring, etc.) [94,100].

Wang et al [123] indicated a notable increase of the bone-implant contact and gene expression levels of the bone attached to TiO_2 NT, while von Willmowski et al [75] reported that osteocalcin expression has increased the most for TiO_2 nanotubes with a diameter of 70 nm when TiO_2 NTs of different diameters (15-100 nm) were implanted in a pig skull.

2.4 Deposition methods used for hydroxyapatite coatings

Surface modifications of the metallic implants with coatings have the role of avoiding an unwanted response from the host, reducing the bacterial adhesion and the immediate inflammatory reaction, as well as increasing the osseointegration capacity and tissue adhesion of the implants.

In order to improve the biological performance and biocompatibility of the metallic implants, they are usually biofunctionalized with calcium phosphates-based coatings (CaP), of which the most known is hydroxyapatite (HAp, $Ca_{10}(PO_4)_6(OH)_2$) due to its similarity to its counterpart found in the inorganic phase of the hard tissues - stoichiometric HAp - which presents a Ca/P ratio of 1.67.

The **electrochemical methods** are versatile methods, which allows the preparation of hydroxyapatite-based coatings, undoped or doped with different types of biocompatible elements, in order to biofunctionalize the metallic biomaterials [7,136,137]. The electrochemical deposition is a relatively fast process, which can be carried out even at low temperatures and which lead to the formation of uniform layers that are covering the entire surface exposed to the electrolyte. At the same time, it should be mentioned that these methods are also feasible for metallic substrates with complex geometries [7,46], this being a great advantage of this method compared to other types of deposition.

Generally, the electrochemical depositions can be performed by using the following techniques [7,136,141,142]: the **potentiostatic/potentiodynamic technique, galvanostatic technique, pulsed technique.**

Part II

Chapter 3. Materials, analysis methods, materials characterization and testing

3.1 The objectives of the doctoral thesis

The general objective of the doctoral thesis aimed to improve the osseointegration properties of titanium by developing nanostructured surfaces with titanium dioxide nanotubes and coating them with a hydroxyapatite layer with enhanced properties in terms of electrochemical behavior, bioactivity, biocompatibility and antibacterial efficiency. To achieve this purpose, a series of specific objectives were necessary:

1. Development of nanostructured surfaces on pure titanium, that are made of titanium dioxide nanotubes with a crystalline structure, with a nanotube diameter of approximately 70 nm, and which can improve the wettability and the corrosion resistance properties;
2. Evaluating the influence of Mg concentration on the physico-chemical characteristics, in order to select the hydroxyapatite-based coatings doped with Mg in optimum concentration, which will be further used to coat the nanostructured surfaces;
3. Obtaining of hydroxyapatite-based coatings doped with Mg or Zn in different concentrations on the nanostructured titanium surface;
4. Physico-chemical and structural investigations of the hydroxyapatite-based coatings doped with Mg or Zn in different concentrations on the nanostructured surface and their selection for further testing;
5. Testing the hydroxyapatite-based coatings doped with Mg or Zn on the nanostructured surface which were selected after the complex investigations, in order to evaluate the electrochemical behavior, bioactivity, biocompatibility and the antibacterial activity.

3.2 Materials

In the present doctoral thesis, pure titanium was used to biofunctionalize its surface, with the aim to transform its *inert* character into a *bioactive* one, at the interface with human hard tissues. In the preliminary tests, which aimed to identify the amount of doping element that can be added in the hydroxyapatite (HAp) structure, as coatings, in order to adjust/control its properties to be used in medical applications, a Ti alloy, namely Ti6Al4V-ELI (Titanium grade 5), was used.

The surface of the Ti discs used in the surface nanostructuring method, and subsequently used as a substrate for the bioactive hydroxyapatite-based coatings, as well as that of the Ti6Al4V alloy discs, which were used as a substrate in the preliminary depositions of hydroxyapatite-based coatings, were prepared as follows: (i) grinding on silicon carbide (SiC) metallographic paper of different grits, which varies in the range of 200 – 1200, (ii) polishing with alumina (Al_2O_3) slurry with a particle size of 1 μm, which has led to a surface with a metallic luster appearance, (iii) cleaning and degreasing in acetone, with a ultrasonic cleaner (Bandelin) for 30 minutes and then rinsed with ultrapure water.

High purity chemical reagents manufactured by Sigma-Aldrich and Merk were used to prepare all the electrolytes used in the surface modification methods, and as testing media of the newly developed surfaces. For the preparation, but also for cleaning/rinsing the experimental samples, two types of water were used according to ASTM D1193-06(2018) (Technical specifications for water used as a reagent): Type I – ultra pure water and Type III – deionized water. A Direct-Q3 UV Water Purification System manufactured by Millipore-Merk was used to prepare these two types of water.

To replicate the conditions, in which the medical devices exert their function in the human body, acellular media can be used to test the *in vivo* behavior. Such media are: the synthetic

body fluid (SBF) proposed by Kokubo [147], artificial saliva (SA) or phosphate buffer solution (PBS), which is also used in cell biology.

3.3 Analysis and characterization methods

The developed nanostructured surfaces and the bioactive coatings studied in the present doctoral thesis were analyzed to determine: the surface morphology; elemental composition; chemical bonds, phase composition, texture and crystallite dimension, mechanical properties; roughness; layer thickness; adhesion; the wettability properties and the surface energy.

Chapter 4. Preliminary studies regarding the development of the nanostructured surfaces and the electrochemical deposition

4.1 Introduction

In order to obtain the nanostructured surfaces with titanium dioxide nanotubes (NT-TiO$_2$) whose properties are adapted to the clinical requirements in terms of crystalline structure and the nanotubes diameter, several experiments were carried out in order to achieve these goals. Preliminary studies were also carried out regarding the electrochemical deposition of Mg-doped HAp, in order to identify the amount of the doping element which can be added in the HAp structure, to adjust/control its properties, in order to be used in medical applications.

4.2 Development and characterization of the nanostructured surfaces with TiO$_2$ nanotubes

In this doctoral thesis, the anodic oxidation process was initially optimized by selecting the process parameters and modifying the anodization time, thus three-time intervals of 30, 60 and 120 minutes, respectively, were selected.

Recent scientific studies, as well as a synthetic analysis of the implantable medical devices market, converge towards the idea, that the bioactivation of titanium with NT-TiO$_2$ with a diameter of about 70 nm, improves the osseointegration capacity and biocompatibility of Ti-based biomaterials used in medical applications [170,171] .

4.2.1 Development of the nanostructured surfaces

4.2.1.1 Samples preparation

The pure Ti samples in the form of discs, whose surface was prepared according to the method described in §3.1, were used in the surface nanostructuring treatment (anodic oxidation).

4.2.1.2 Anodic oxidation

Growth of the TiO$_2$ nanotubes on the cp-Ti surface by anodic oxidation, was carried out in the presence of an electrolyte solution with a concentration of 0.5 wt% HF. The anodic oxidation process was carried out at a constant potential of 20 V for 120 min, 60 min, and 30 min, respectively, at room temperature, with a direct current source (Keysight DC N5771A) [48, 49,102]. After the anodic oxidation stage, the samples were rinsed with ultrapure water and dried in hot air. In Table 4.1. are presented the samples codification, along with the selected parameters.

Table 4.1. Sample codification and electrochemical parameters

Material	Sample codification
cp Ti polished	Ti-L
cp Ti anodized for 120 min	NT-120
cp Ti anodized for 120 min and annealed	NT-120 (TT)
cp Ti anodized for 60 min	NT-60
cp Ti anodized for 60 min and annealed	NT-60 (TT)
cp Ti anodized for 30 min	NT-30
cp Ti anodized for 30 min and annealed	NT-30 (TT)

4.2.1.3 Annealing treatment

For this structural modification, a heat treatment at a temperature of 450 °C for 2 hours was performed, by using a heat treatment furnace (Nabertherm, Germany), while the cooling was performed in air.

4.2.2 Characterization of the nanostructured surfaces

After obtaining the nanostructured surfaces, they were characterized in terms of morphology, elemental and phasic composition, being also highlighted the surface characteristics such as roughness, wetting degree and corrosion resistance.

4.2.2.1 Morphology

Figure 4.3 shows the morphology of the surfaces obtained after anodic oxidation, and the annealing treatment applied afterwards. The nanostructured surface consists of titanium dioxide nanotubes (NT-TiO$_2$) aligned, vertically oriented and hollow, which can be described as parallel tubular structures, uniformly distributed over the entire surface.
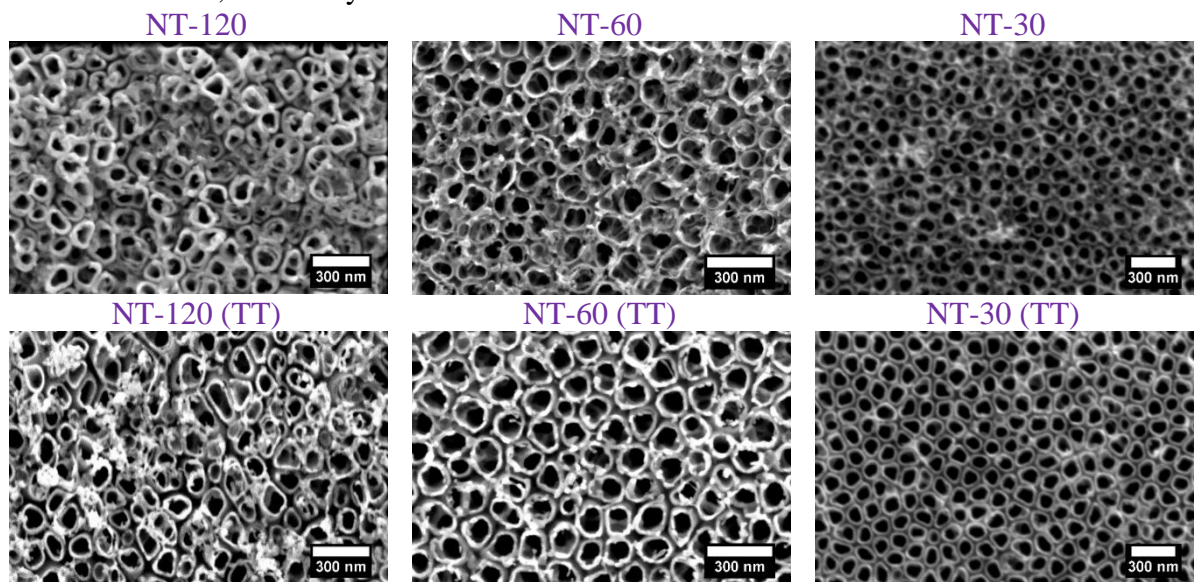
Figure 4.3. *SEM images of the surface morphology after the anodic oxidation for 120, 60 and 30 min., and annealing treatment*

By using the acquired HR-SEM images and the image processing software, *Image J*, the diameters of the nanotube were measured (Table 4.3 and Figure 4.5). According to this analysis, it was noted that for all surfaces, the heat treatment has led to a slight decrement of the nanotube's diameter, to a value of approx. 70 nm (from a maximum of approx. 130 nm), as well as to a better organization.

Table 4.3. *The diameter of the nanotubes obtained as a function of the applied anodization time*

Samples	NT diameter (nm)
NT-120	128.25 (±10,96)
NT-120 (TT)	120.19 (±13.37)
NT-60	77.67 (± 15.94)
NT-60 (TT)	75.81 (± 10.89)
NT-30	75.27 (± 15.76)
NT-30 (TT)	70.08 (±11.67)
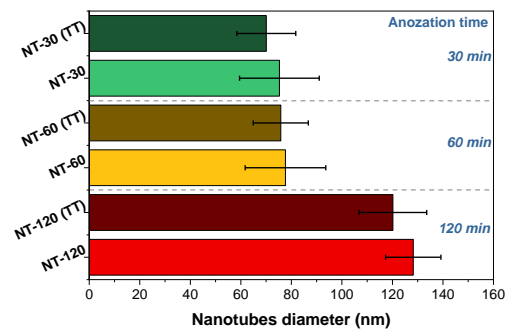
Figure 4.5. *The diameter of the nanotubes obtained as a function of the applied anodization time*

4.2.2.2 Elemental composition

The chemical composition obtained by EDS analysis revealed the presence of the main components of the oxide layer and the base material, namely oxygen (O) and titanium (Ti). According to the EDS analysis performed on the surface of the anodically oxidized experimental samples, an increase in the oxygen concentration and a decrease in that corresponding to titanium can be observed, independent of the anodic oxidation time, suggesting that the thickness of the titanium oxide layer has increased after the thermal treatment.

4.2.2.3 Phasic composition

As it can be seen (Figure 4.8), irrespective of the selected anodization time, before the annealing treatment, the titanium dioxide (TiO$_2$) presents an amorphous structure, being identified as the main Ti phase (according to ICDD # 04-007-9313), which was used as the base material.

After applying the annealing treatment, one can observe the appearance of some diffraction peaks characteristic to the TiO$_2$ crystalline phases, namely, anatase according to ICDD standard #021-1272 as the main phase, as well as some diffraction peaks specific to rutile (ICDD #021-1276).

Figure 4.8. *Diffractograms of the developed nanostructured surfaces, before and after thermal treatment*

Following the obtained results and the preconditions necessary for the selection of nanostructured surfaces with TiO$_2$ nanotubes whose diameter should not exceed 80 nm, it was considered that the surfaces obtained by anodic oxidation at 120 minutes should no longer be considered in the present study.

4.2.2.4 Roughness

In Table 4.6., the main roughness parameters, Ra, Rq and the asymmetry factor, R_{Sk}, obtained from the measurements, are presented. The polished surfaces whose values can vary between 0.1 μm and 3 μm [185], recorded values of approx. 82 nm of the Ra parameter. It is observed that after the anodic oxidation process, the most important parameter characterizing the roughness (Ra), shows a significant increment, which after the thermal treatment began to decrease.

Table 4.6. *The average values of the parameters characterizing the roughness of the obtained surfaces (Ra, Rq and R_{Sk})*

Sample	Ra (nm)	Rq (nm)	R_{Sk}
Ti-L	81.7 (± 11.4)	103.2 (± 13.4)	0.05 (± 0.01)
NT-60	266.8 (± 19.1)	335.1 (± 25.2)	0.12 (± 0.03)
NT-60 (TT)	186.3 (± 9.1)	234.6 (± 10.8)	-0.13 (± 0.05)
NT-30	159.8 (±12.8)	198.34 (±14.7)	0.20 (± 0.04)
NT-30 (TT)	128.2 (±12.1)	161.48 (±16.9)	0.17 (± 0.03)

4.2.2.5 Wettability

Wettability is an important factor, that plays an essential role in the biocompatibility and functionality of implants. Figure 4.10 shows the results obtained from the contact angle measurements for the developed surfaces, as well as the images with the shape of the SBF droplets, in contact with the investigated surfaces. It can be observed that none of the surfaces
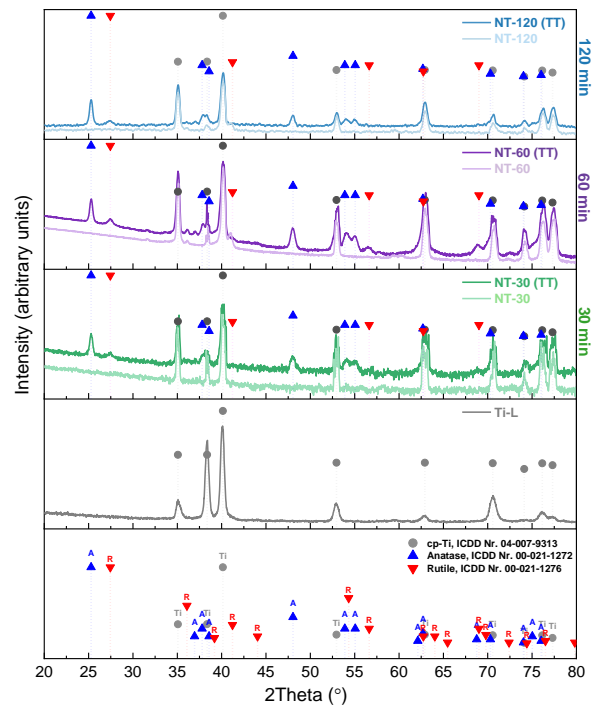
have a contact angle higher than 90°, indicating a hydrophilic surface with high surface energy, suggesting that the liquid will spread on the solid surface.
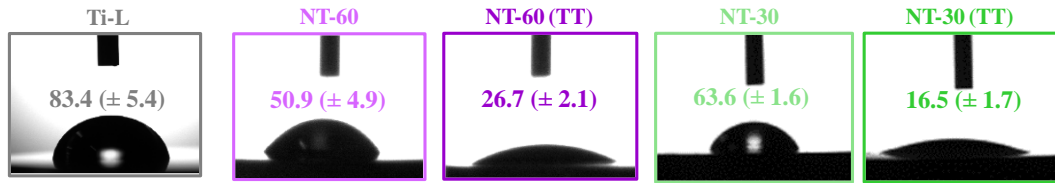
Ti-L	NT-60	NT-60 (TT)	NT-30	NT-30 (TT)
83.4 (± 5.4)	50.9 (± 4.9)	26.7 (± 2.1)	63.6 (± 1.6)	16.5 (± 1.7)

Figure 4.10. *Contact angle values for the polished Ti surface and nanostructured surfaces*

As a general conclusion, it can be said that the anodic oxidation treatment makes the new nanostructured surfaces to present a more hydrophilic character, compared to the initial (polished) surface, with the lowest value of the contact angle and thus the highest wettability, being recorded for the surface obtained at an anodizing time of 30 min., followed by annealing treated (NT-30 (TT)).

4.2.2.6 Corrosion resistance

It is well known that a material exhibits good corrosion resistance if it has a more electropositive corrosion potential (E_{corr}), a low corrosion current density (i_{corr}) and a high polarization resistance (Rp) [158,186]. Figure 4.12 shows the Tafel plots and Table 4.7 presents the main parameters of the electrochemical corrosion process obtained from the corrosion resistance tests carried out in SBF.
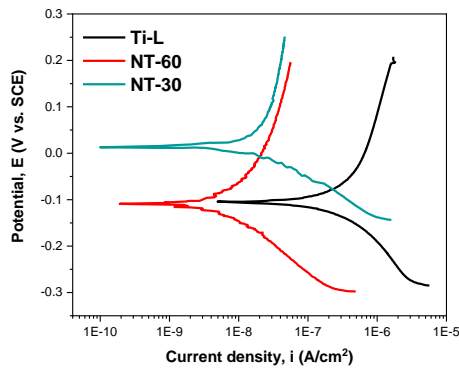
Figure 4.12. *Tafel plots of the investigated samples*

Table 4.7. *Electrochemical parameters specific for the investigated surfaces (E_{corr} – corrosion potential, i_{corr} – corrosion current density, Rp – polarization resistance, CR – corrosion rate)*

Sample	E_{corr} (mV)	i_{corr} (nA/cm^2)	β_c (mV)	β_a (mV)	Rp (kΩxcm^2)	CR (μm/an)
Ti-L	- 105	684.32	242,56	839,50	119.56	5.96
NT-30 (TT)	-133	68.78	94,165	837,312	547.16	0.58
NT-60 (TT)	- 109	11.143	136.63	421.80	4,026.83	0.01

Thus, by taking into consideration the criteria stated above, it can be said that titanium nanostructured surfaces with TiO$_2$ nanotubes exhibits better corrosion resistance in SBF compared to the polished one (Ti-L).

4.3 Development and characterization of the osteoconductive coatings

In this section, are presented the preliminary studies which have been carried out to obtain the Mg-doped HAp by electrochemical deposition, in order to identify the doping element amount which can be added to the HAp structure, so that the properties can be adjusted/controlled, with the aim to be used in medical applications.

4.3.1 Development of the osteoconductive coatings

4.3.1.1 Electrochemical deposition in pulsed mode

The titanium alloy metallic substrate, in the form of disks with $\Phi = 20$ mm and $h = 2$ mm was used as working electrode. The electrochemical depositions were carried out in a standard electrochemical cell with three electrodes, respectively: working electrode (WE) – Ti6Al4V, reference electrode (RE) – Calomel electrode, and auxiliary electrode (AE) – platinum electrode, with the help of a PARSTAT MC potentiostat/galvanostat (Princeton Applied Research - Ametek), by using the pulsed galvanostatic technique [141].

The samples codification can be found in Table 4.8. The parameters specific to the electrochemical technique in pulsed mode are presented in Table 4.9. The chemical composition of the electrolytes used to obtain HAp-based coatings is presented in Table 4.10. The electrolytes were prepared so that the (Ca+Mg)/P ratio, to be similar to stoichiometric hydroxyapatite of 1.67.

Table 4.8. *Samples codification for the undoped and Mg doped HAp coatings*

Material	Samples codification
HAp	H
HAp doped with 1.05 mM Mg	H-Mg1
HAp doped with 1.575 mM Mg	H-Mg1.5
HAp doped with 2.10 mM Mg	H-Mg2

Table 4.9. *Electrochemical parameters used to obtain the undoped and Mg doped HAp coatings*

Samples codification / Deposition parameters		H; H-Mg1; H-Mg1.5; H-Mg2
Cycle	i_{ON} (mA/cm^2); t_{ON} (s)	- 0.85 mA/cm^2; 1 s
	i_{OFF} (mA/cm^2); t_{OFF} (s)	0 mA/cm^2; 1 s
Number of cycles		1200 cycles
Deposition time		40 min.
Temperature		75 °C

Table 4.10. *Chemical composition of the electrolytes used to obtain the undoped and Mg-doped HAp coatings*

Substrate	Coating	Sample codification	Chemical composition (mM)			pH
			Ca(NO$_3$)$_2\cdot$4H$_2$O	NH$_4$H$_2$PO$_4$	Mg(NO$_3$)$_2\cdot$6 H$_2$O	
Ti6Al4V	HAp	H	10.500		-	
	HAp+Mg	H-Mg 1	9.450	6.25	1.050	5 (ajustat cu 1 M NaOH)
		H-Mg1.5	8.925		1.575	
		H-Mg2	8.400		2.100	

4.3.2 Characterization of the osteoconductive coatings

The obtained experimental samples were investigated in terms of morphology, elemental and phasic composition, roughness, adhesion, and electrochemical behavior, focusing on the Mg concentration and its influence on the HAp characteristics. In the case of the H-Mg2 sample, it was observed that the coating is not uniform, this being the reason why it wasn't further used in the tests.

4.3.2.1 Morphology

The SEM images presented in Figure 4.15, are emphasizing the coatings morphology. The undoped HAp (H) coatings present a morphology made of long and thin crystals, similar to a ribbon, which was also met in other studies [190,191]. Comparing the H-Mg and H coatings, the apatite crystals began to be wider with the addition of Mg, and the increment of its concentration. The obtained results are similar to those presented in a study performed by Bakin et al. [195].
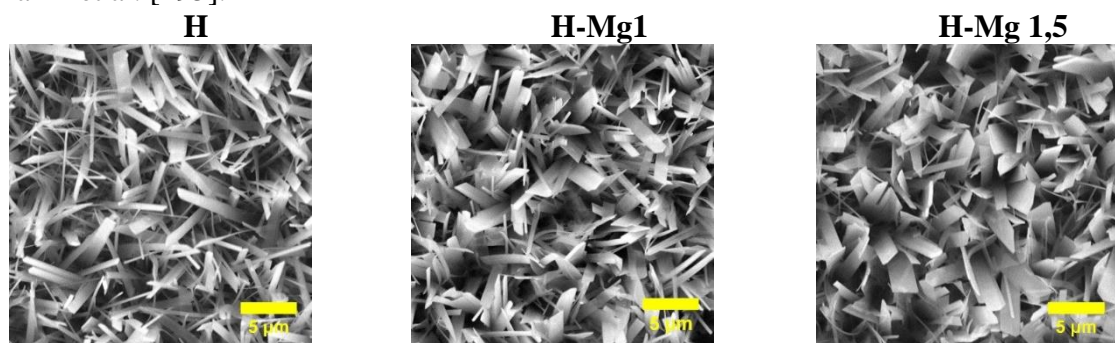
H	H-Mg1	H-Mg 1,5

Figure 4.15. Morphology of the undoped hydroxyapatite coatings (H) and doped with Mg in different concentrations (H-Mg1 and H-Mg1.5) [141]

4.3.2.2 Elemental composition

The EDS analysis of the coatings has confirmed the presence of the elements specific to calcium phosphates (Ca and P), as well as the doping element (Mg), these also being uniformly distributed on the entire analyzed area. The (Ca+Mg)/P ratio calculated for the experimental coatings is 1.59 for the H and H-Mg1 coatings, noting that for the H-Mg1.5 coatings, this value slightly decreases to 1.56, indicating that the doping process above a certain concentration leads to formation of a Ca-deficient apatite, most likely generated by the defects appeared following the ionic substitution [196].

4.3.2.3 Phasic composition

The X-ray diffractograms of the undoped and Mg-doped HAp based coatings are shown in Figure 4.18. The coatings show the specific diffraction peaks of HAp, according to ICDD standard #09-0432. It can also be observed that the strongest relative intensity was recorded for the (002) plane at an angle of $2\theta = 25.95°$.

In the detailed diffractogram from Figure 4.18, it can be seen that with the addition of Mg in HAp, the diffraction peak associated to the (002) plane slightly shifted to higher angles for the H-Mg1 and H-Mg1.5 coatings. These findings are in good correlation with other studies and suggests, that Mg ions have replaced part of the Ca ions from the HAp structure [204,205].

It should also be noted that the presence of Mg in its metallic form, was not identified, indicating that Mg is present in the coatings, only as ions.

In the case of H coatings, the crystallite size shows a value of 8.4 nm, which with the addition of Mg has increased to a value of 8.8 and 10.4, respectively, for H-Mg1 and H-Mg1.5 coatings. Regarding the crystallinity,

Figure 4.18. Diffractograms of the hydroxyapatite-based coatings undoped and doped with Mg in different concentrations

it was observed that addition of Mg in the HAp structure has led to an improvement of the coating's crystallinity, from a value of ~18% for the H coatings, to a maximum of ~30% for H-Mg1 coatings. A lower crystallinity was noted for the coatings with a higher Mg concentration, of ~27%. In conclusion, based on XRD investigations, it can be mentioned that the crystallinity of HAp-based coatings increases with the addition of Mg.

4.3.2.4 Roughness

As it can be observed from Table 4.11, both the Ra and the Rq parameter have increased with the addition of Mg in HAp. By increasing the Mg concentration in the electrolyte used to obtain the coatings, from 1 to 1.5 mM, it can be seen that the Ra parameter has increased by ~ 8 times, passing from the nanometric scale for the H and H-Mg1 coatings, to the micrometric one, for the H-Mg1.5 coatings. According to the scientific literature, the average roughness value (Ra) of the commercial dental implants is found to be in the range of 0.1 – 10 μm [206]. Thus, it can be noted that the experimental coatings, fall within this range.
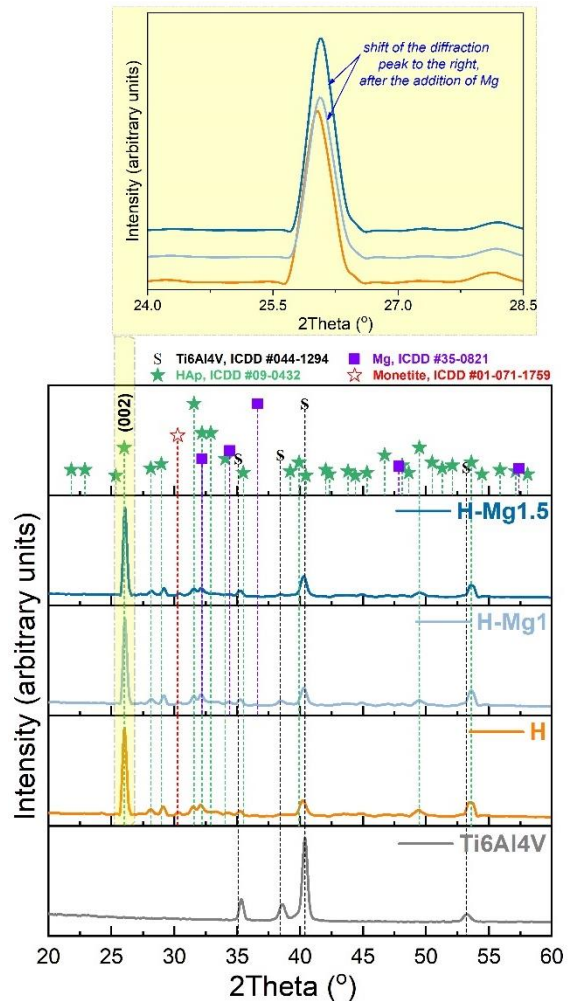
Table 4.11. *The main roughness parameters (Ra, Rq şi R_{Sk})*

Material	Ra (nm)	Rq (nm)	R_{Sk}	Coating thickness (µm)
H	439.7 (±33.9)	587.9 (±66.7)	0.84 (±0.1)	11.1 (±0.9)
H-Mg1	558.2 (±37.9)	710.9 (±47.0)	0.38 (±0.1)	12.2 (±0.7)
H-Mg1.5	4,396.9 (±895.4)	6,609.1 (±1,071.4)	2.44 (±0.25)	10.5 (±0.7)

According to the obtained results, it can be observed that the lowest layer thickness, of 10.5 µm, was registered for the H-Mg1.5 coatings, followed by the H and H-Mg coatings, which have registered thicknesses of ~ 11 and ~ 12 µm, respectively. The differences among the values obtained for the layer thickness, can be associated with the deposition rate, which is influenced by the amount of Mg added in the electrolyte.

4.3.2.5 Adhesion

Figure 4.22 shows the SEM images of the imprints/scratches left after the adhesion testing by tape test, according to the ASTM D3359-17 standard procedure.
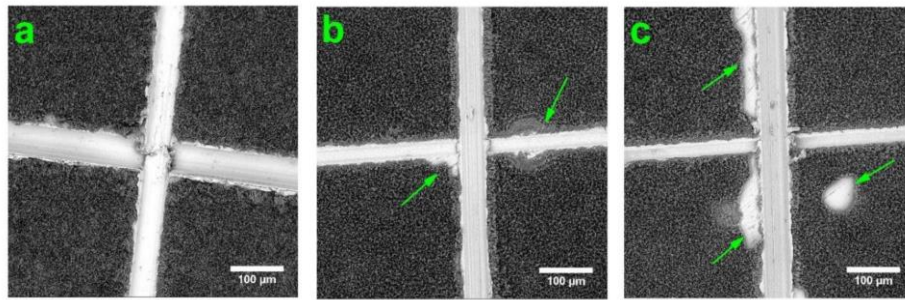
Figure 4.22. *SEM images of the (a) hydroxyapatite – H, (b) Mg-doped hydroxyapatite – H-Mg1 and (c) Mg-doped hydroxyapatite – H-Mg1.5 coatings, after adhesion tests (green arrows indicate the affected areas/ delaminated)[141]*

The adhesion results (Table 4.12) were classified into the following categories: 5B (0%) for H coatings, and 4B, for H-Mg1 coatings, because at the intersection areas of the grids, small areas with detachments from the coatings in a percentage of 1.24%, were identified. As the amount of Mg increases, it can be seen that some delamination's are not only at the intersection, but also along the imprints, thus being assigned a score of 3B, since 9.55% of the surface is affected.

Table 4.12. *Evaluation of the coating's adhesion to the substrate according to ASTM D3359-17*

	H	H-Mg1	H-Mg1.5
Affected/delaminated surface (%)	*0 %*	*1.24 %*	*9.55 %*
Adhesion according to ASTM D3359-17	*5B*	*4B*	*3B*

Therefore, the adhesion tests revealed that most of the coating remains on the substrate, regardless the coating type, and by increasing the Mg amount the adhesion starts to decrease.

4.3.2.6 Electrochemical behavior

The open circuit potential curves and Tafel plots for the undoped and Mg-doped HAp coatings are shown in Figure 4.23. Based on Tafel extrapolation, the main electrochemical parameters were extracted, and are presented in Table 4.13.

16

(a)　　　　　　　　　　　　　　　　　　(b)

Figure 4.23. *Evolution of the open circuit potential (a) and Tafel plots (b) for the investigated coatings*

Table 4.23. *The main electrochemical parameters obtained for the investigated coatings (E_{OC} – open circuit potential, E_{corr} – corrosion potential, i_{corr} – corrosion current density, Rp – polarization resistance)*

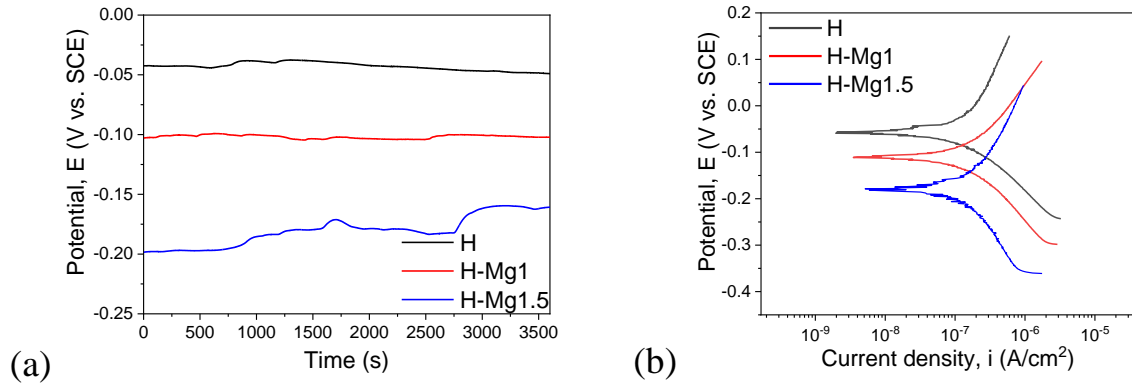| Material	H	H-Mg1	H-Mg1,5
E_{oc} **(mV)**	−48.9 (±5.2)	−102.2 (±7.8)	−160.70 (±9.4)
E_{corr} **(mV)**	−56.9 (±6.3)	−110.3 (±9.1)	−180.50 (±10.7)
i_{corr} **(nA/cm^2)**	22.45 (±3,82)	53.70 (±4.56)	90.43 (±6.75)
β_c **(mV)**	34.23 (±5.51)	63.22 (±9.47)	100.33 (±12.34)
β_a **(mV)**	35.98 (±6.15)	60.67 (±8.77)	105.39 (±11.92)
R_p **(kΩ·cm^2)**	339.70 (±10.42)	250.67 (±11.13)	247.11 (±12.58)

Thus, the obtained results underline that the addition of Mg leads to the modulation of the electrochemical behavior, and implicitly, the solubility/biodegradation of HAp. These observations are in good correlation with a study performed by Cai et al. [210], in which it was observed that by increasing the Mg content, a higher degradation rate of the HAp can be obtained.

4.3.3 Conclusions

In conclusion, the properties and characteristics of HAp obtained by pulsed galvanostatic electrochemical deposition, can be controlled by addition of Mg in different concentrations, and thus, bioactive ceramic biomaterials with adjustable properties that can be used in medical applications, can be obtained.

Chapter 5. Experimental results regarding the characterization of the new osteoconductive surfaces

5.1 Development of the osteoconductive coatings deposited on the nanostructured surfaces

The HAp based coatings were achieved on Ti substrate (cp-Ti grade 2) nanostructured with titanium dioxide nanotubes, obtained by anodic oxidation for 30 minutes and annealed at 450°C, in similar conditions as the one presented in § 4.1.1.2. The preparation protocol of the HAp-based coatings on nanostructured substrate was carried out similarly to the one presented in § 4.3.1.

In Table 5.1. are presented the samples codification used in the current chapter of the doctoral thesis. The chemical composition of the electrolytes used to obtain the undoped HAp-based coatings and the ones doped with Mg or Zn in different concentrations, are presented in Table 5.2.

The electrolytes were prepared so that the ratio (Ca+M)/P, where M=Mg or Zn in different concentrations, to be similar to that of stoichiometric hydroxyapatite (HAp), of 1.67 [48,49].

Table 5.1. *Sample codification of the HAp coatings undoped and doped with Mg or Zn*

No.	Description	Codification
1	Nanostructured surface with titanium dioxide	*NT*
2	Undoped hydroxyapatite electrochemically deposited on titanium dioxide nanostructured surface	*H*
3	Hydroxyapatite with 1 mM of Mg in the electrolyte, electrochemically deposited on titanium dioxide nanostructured surface	*H-Mg1*
4	Hydroxyapatite with 1.5 mM of Mg in the electrolyte, electrochemically deposited on titanium dioxide nanostructured surface	*H-Mg2*
5	Hydroxyapatite with 0.015 mM of Zn in the electrolyte, electrochemically deposited on titanium dioxide nanostructured surface	*H-Zn1*
6	Hydroxyapatite with 0.020 mM of Zn in the electrolyte, electrochemically deposited on titanium dioxide nanostructured surface	*H-Zn2*

Table 5.2. *Chemical composition of the electrolytes used to obtain the undoped and Mg- or Zn-doped HAp based coatings*

Substrate	Coating	Sample codification	Chemical composition (mM)				pH
			$Ca(NO_3)_2$ $\cdot 4H_2O$	$NH_4H_2PO_4$	$Mg(NO_3)_2$ $\cdot 6 H_2O$	$Zn(NO_3)_2$ $\cdot 6H_2O$	
NT	**HAp**	**H**	10.000		0	0	5 (adjusted with 1 M NaOH)
	HAp+Mg	**H-Mg1**	9.000	6	1.000	0	
		H-Mg2	8.500		1.500	0	
	HAp+Zn	**H-Zn1**	9.985		0	0.015	
		H-Zn2	9.980		0	0.020	

5.2 Characterization of the osteoconductive coatings deposited on nanostructured surface

The obtained experimental samples were investigated in terms of morphology, elemental and phasic composition, chemical bonds, roughness, adhesion and surface energy, emphasizing the concentration of the doping element, Mg or Zn, and their influence on the characteristics of HAp.

5.2.1 Morphology

In Figure 5.2. are presented the SEM images with the morphologies of the undoped HAp and doped with Mg or Zn in different concentrations. Thus, it can be noted that all coatings present a morphology that consists in ribbon-like crystals, which are covering the entire surface exposed to the electrolyte during the electrochemical deposition. With respect to the doping element used (Mg or Zn) and its concentration in the electrolyte, some differences regarding the morphological aspect, were observed [48,49].

H-Zn1   **H-Zn2**
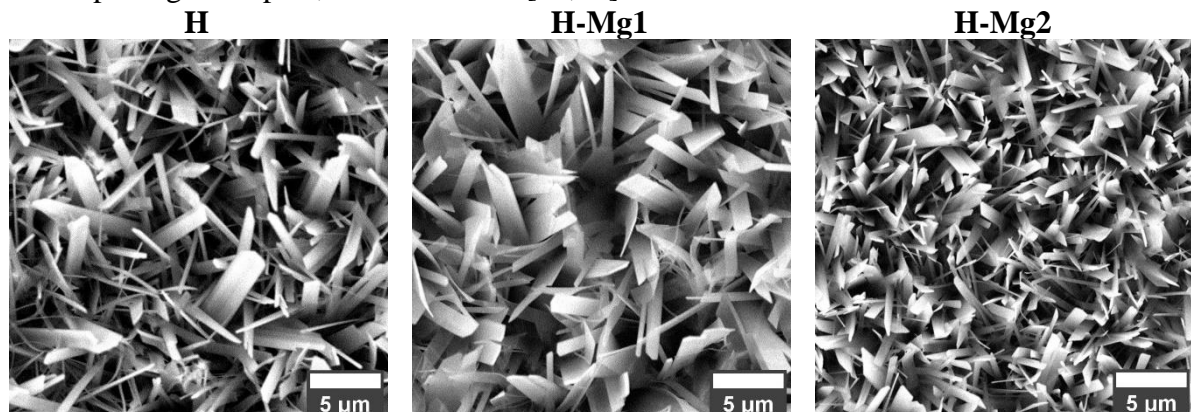
Figure 5.2. SEM images of the undoped and Mg- or Zn-doped HAp-based coatings in different concentrations

The obtained HAp-based coatings present a uniform aspect and depending on the doping element and its concentration in the electrolyte used during deposition, the following aspects were observed:

• compared to undoped HAp (H), the **H-Mg coatings** show minor changes in terms of morphology, and as seen in Figure 5.2, addition of a concentration of 1 mM in the electrolytic solution, leads to a slight increment of the ribbons, which became a little wid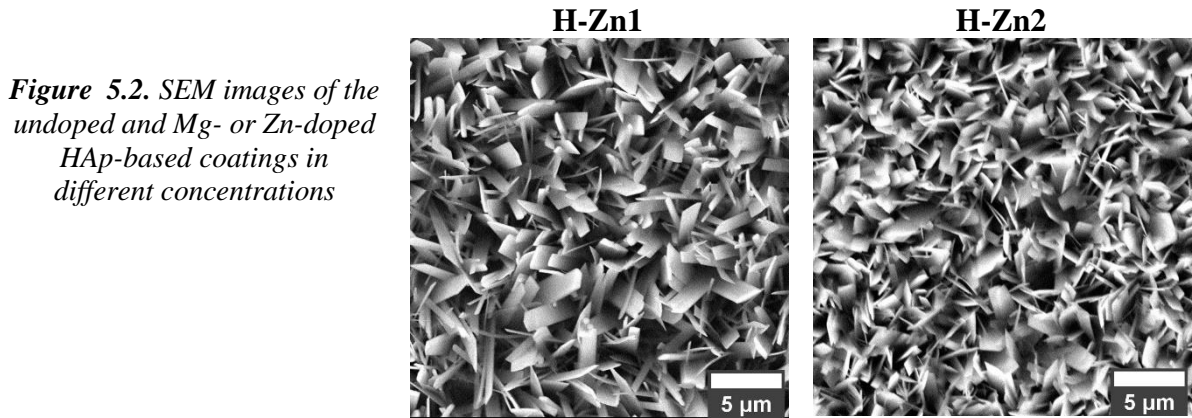er, while still remaining thin; increasing the concentration towards a value of 1.5 mM in the electrolyte, leads to a visible decrease of the ribbons dimensions, which present much smaller widths, compared to the H and H-Mg1 coatings;

• compared to H and H-Mg1 coatings, **H-Zn coatings** show much smaller ribbons in terms of width, which decreases by increasing the Zn concentration.

Regarding the formation mechanism of the HAp-based coatings obtained by electrochemical deposition, Figure 5.3 highlights that the coatings obtained in the present doctoral thesis consists in two layers which present different morphologies. The first layer is obtained in the first part of the electrochemical deposition process, and is made of plate-like crystals, which generates a more compact appearance, and a smaller thickness of the coating, compared to the second layer, which presents a higher thickness, and is made of longer and thinner ribbon-like crystals, grown perpendicular to the surface of the metallic substrate.
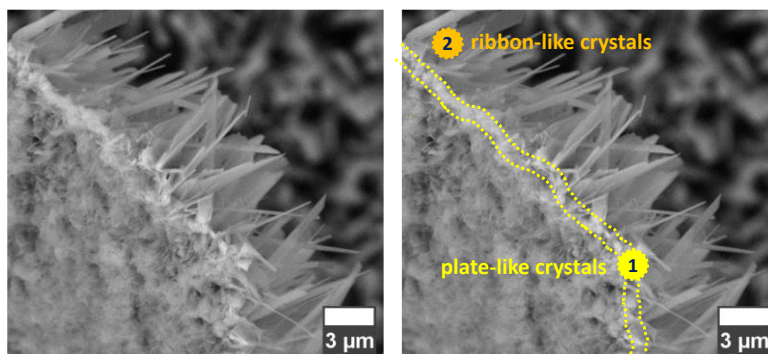
Figure 5.3. Representative SEM image of the Mg-doped HAp (H-Mg2) coating in section, without and with annotations [49]

5.2.2 Elemental composition

Table 5.4 shows the chemical composition obtained by EDS analysis of the coatings prepared through pulsed galvanostatic technique. Based on the obtained results, the Ca/P ratio was calculated with, and without, the doping element (Mg or Zn).

According to these results, it can be seen that the (Ca+M)/P ratio decreases with the addition of the doping elements, from a value of 1.59 obtained for H coatings, to a value of 1.57 and 1.56 for H-Mg1 and H-Mg2 coatings, and to values of 1.56 and 1.55 for H-Zn1 and H-Zn2 coatings, respectively.

In terms of the doping element concentration in the obtained coatings, it must be stated that a concentration of $Zn \leq 1.2$ wt. %, does not induce a cytotoxic effect, improves cell proliferation and provides a good antibacterial effect [214,215]. At the same time, Mg is found

in hard bone tissues in a concentration of 0.32 – 0.78 wt.%, and in this case, it can be noted that both layers of HAp doped with Mg, present a concentration of Mg within this range.

Table 5.4. *Chemical composition (at.% and wt.%) of the HAp based coatings undoped and doped with Mg or Zn in different concentration, deposited on nanostructured substrate*

Material	Elemental composition								Ratio Ca/P	Ratio (Ca+M)/P
	Ca		P		Mg		Zn			
	(at.%)	(wt.%)	(at.%)	(wt.%)	(at.%)	(wt.%)	(at.%)	(wt.%)		
H	61.46	67.36	38.54	32.64	0	0	0	0	1.59	1.59
H-Mg1	60.55	66.66	38.89	33.03	0.46	0.31	0	0	1.56	1.57
H-Mg2	60.39	66.43	39.06	33.20	0.55	0.37	0	0	1.55	1.56
H-Zn1	60.21	65.71	39.01	32.90	0	0	0.78	1.39	1.54	1.56
H-Zn2	59.54	64.77	39.16	32.93	0	0	1.30	2.30	1.52	1.55

5.2.3 Phasic composition, texture and crystallite dimension

In Figure 5.8. are presented the X-ray diffractograms obtained for the undoped and Mg- or Zn-doped HAp-based coatings. These were compared to ICDD (International Center for Diffraction Data) standards for the following phases: hydroxyapatite (PDF #09-0432), monetite (PDF #1-071-1759), anatase (PDF #021-1272), titanium (PDF #44-1294), magnesium (PDF #04-006-2605), and zinc (PDF #04-0831).
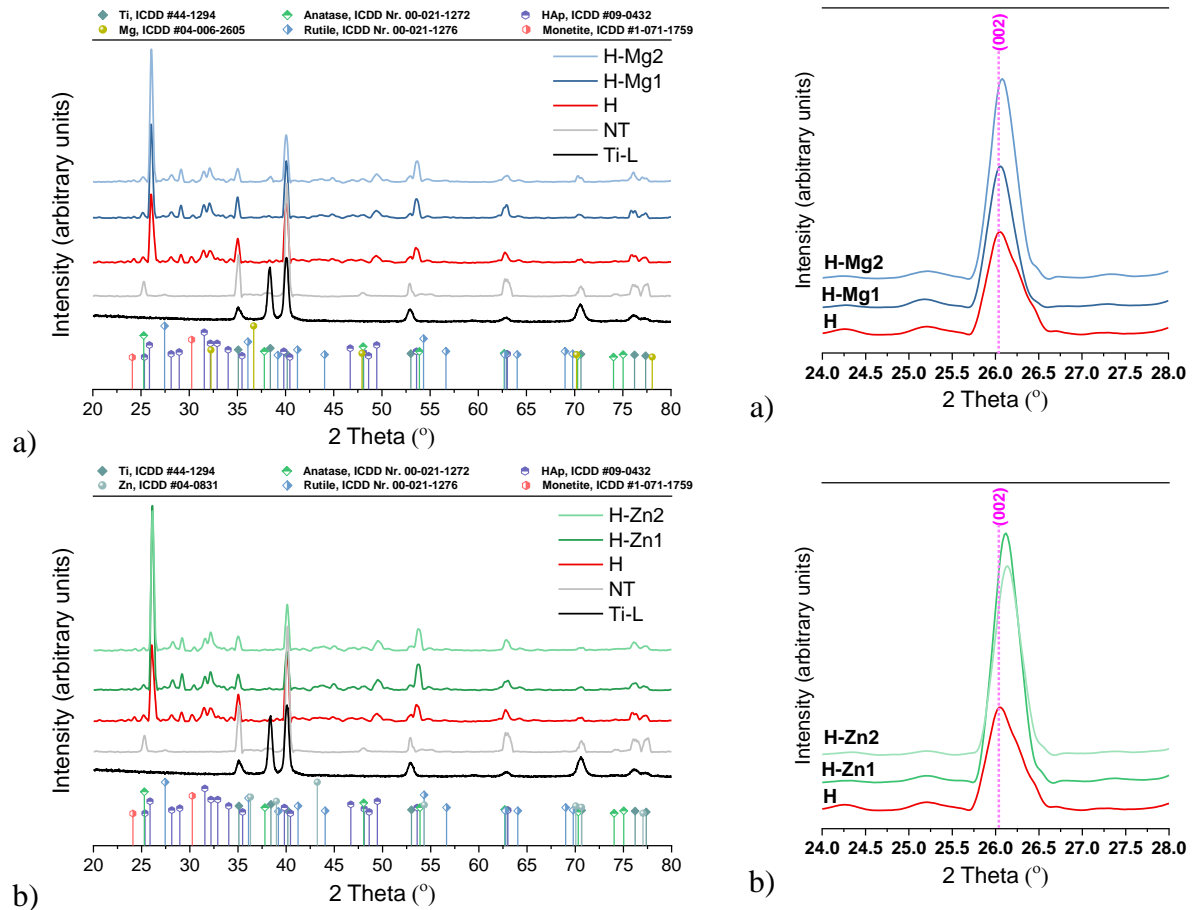
Figure 5.8. *Diffractograms of HAp-based coatings undoped and doped with Mg (a) or Zn (b) in different concentrations*

Figure 5.9. *Section of interest of the X-ray diffractograms for the undoped and Mg (a) or Zn (b) doped HAp-based coatings in different concentrations*

As can be seen in Figure 5.8, the obtained coatings show the diffraction peaks specific to hydroxyapatite (HAp) according to the ICDD standard, No. 09-0432, these being the predominant ones, suggesting that this is the main phase identified in the coatings.

In Figure 5.9 are shown sections of interest of the diffractograms for the diffraction peak associated to the (002) plan. From these diffractograms it can be observed that the diffraction

peak of HAp from ~ 26° related to the (002) plan, changes its intensity and slightly shifts to the right, indicating that Mg^{2+} and Zn^{2+} ions are replacing the Ca^{2+} ones from the HAp structure.

Thus, it can be concluded that the XRD analyses has confirmed the doping with Mg or Zn in different concentrations in the HAp-based coatings through substitution, which is sustained by the modification of the structural parameters (crystallite size, the structural parameters, crystallinity, the shift of the angle $2\theta = \sim 26$ associated to (002) plane towards higher values for).

5.2.4 Chemical bonds

In Figure 5.11. are presented the FTIR spectra of the HAp-based coatings undoped and doped with Mg or Zn in different concentrations, electrochemically deposited on nanostructured surface. Since the coatings are porous, the registered FTIR spectra are noisy.

The vibration bands observed between 600 and 1100 cm^{-1} are attributed to the absorption peaks of the phosphate group (PO_4^{3-}), which are present in all coatings. The FTIR results have demonstrated the formation of the stoichiometric HAp phase on the nanostructured substrates, regardless the nature and/or presence of the doping elements.

Compared to the undoped HAp (H), the Mg or Zn doping elements in different concentrations have led to the decrement of the intensity of these bands for H-Mg2, H-Zn1 and H-Zn2 coatings, while H-Mg1 coatings showed intensities close to those of H [48,49].

a)

b)

***Figure 5.11.** FTIR spectra undoped and Mg (a) or Zn (b) doped HAp-based coatings deposited on the nanostructured surface*

5.2.5 Roughness

Figure 5.13 shows the average values of the parameters ***Ra*** - the value of the arithmetic mean deviation of the roughness profile in relation to the median line, ***Rq*** - the root mean square deviation of the profile, compared to the average value and ***R_{Sk}*** - the asymmetry factor of the evaluated profile) along with their standard deviations.

Following the analysis of the main parameters which are characterizing the roughness (Figure 5.13), it can be observed that:

***Figure 5.13.** The characteristic roughness parameters for HAp-based coatings*

- all coatings show an average roughness (Ra) higher than that of Ti-L (83 nm) and NT (132 nm); in the case of the NT surface, the roughness increment is explained by the presence of the nanotubes on the Ti surface;

- the addition of Mg in a concentration of 1 mM in the electrolyte leads to a slight increase of the Ra parameter from ~536 nm for the H coatings, to 582 nm for H-Mg1, while further
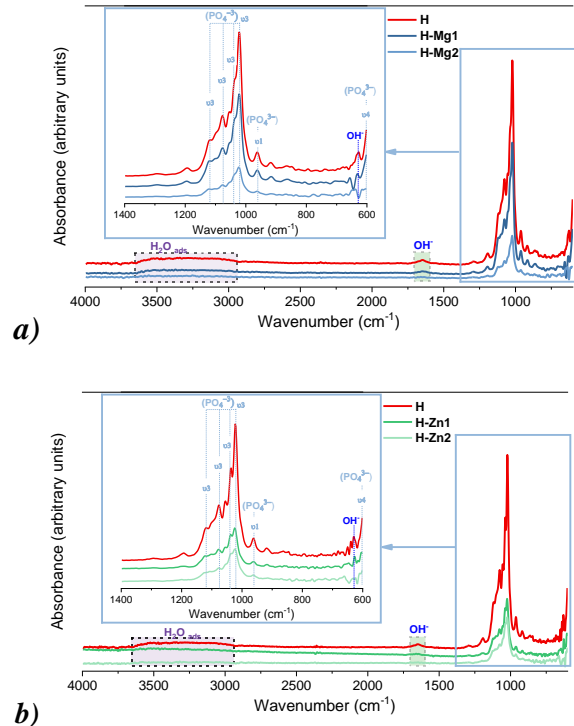
increasing the Mg concentration in the electrolyte has led to the decrement of the roughness towards a value of ~493 nm, which is smaller than the one of H and H-Mg1;

• addition of Zn into the HAp, the value of the arithmetic mean deviation of the roughness profile (Ra) decreases from a value of 536 nm in the case of H coatings, to a value of ~ 320 nm for the H-Zn1 coatings and ~ 242 nm in the case of the H-Zn2 coatings, indicating that as the concentration of Zn in the electrolyte increases from a value of 0.015 mM to 0.020 mM, the roughness decreases.

5.2.6 Coating thickness

Figure 5.14 presents the values of the coating thicknesses obtained for the HAp based coatings undoped and doped with Mg or Zn in different concentrations. The samples coded with H present an average value of the coatings thickness of ~10 μm, while the H-Mg1 and H-Mg2 coatings registered the highest thicknesses, of 11 and 14 μm, respectively. The H-Zn1 and H-Zn2 coatings have registered thicknesses of 10 and 6 μm. According to the scientific literature, a too high thickness leads to a poor adhesion to the substrate, and a smaller

Figure 5.14. *Coating thickness for the HAp based coatings undoped and doped with Mg or Zn in different concentrations*

one leads to a poor stability, thus a layer thickness of ~ 10 µm is considered to be ideal [220]. In conclusion, it can be seen that the coatings with a lower concentration of the doping element as well as the undoped HAp based coatings meet this condition, having thicknesses of approx. 10 µm.

5.2.7 Adhesion

Figure 5.15 shows the SEM images obtained after performing the adhesion test. The "adhesive tape" test demonstrates that the adhesion of the hydroxyapatite coatings undoped and doped with lower amounts of Mg or Zn (H, H-Mg-1, HZn-1) to the titanium substrate with a nanostructured surface with dioxide nanotubes of titanium, falls into a higher category according to the standard used. A slightly weaker adhesion was observed for the coatings doped with a higher amount of the doping element (H-Mg2, H-Zn2) which is positioned in the upper category (3B) of the ASTM D 3359-17 standard.
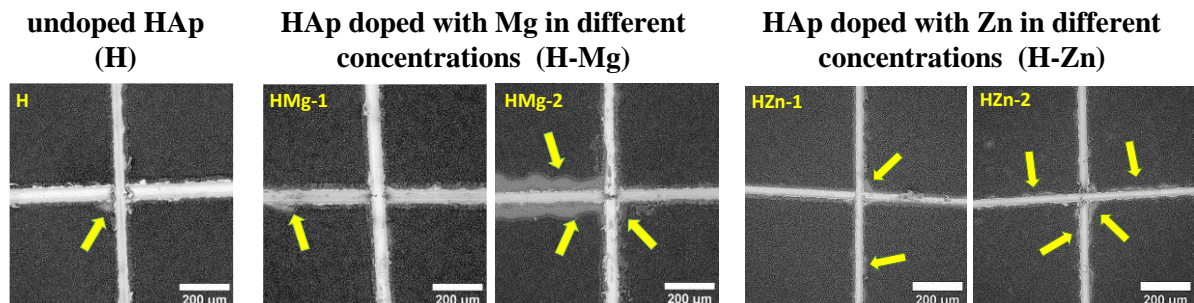
Figure 5.15. *SEM images of the imprint after the adhesion test (yellow arrows indicate areas with delamination/exfoliation)*

Complementary to the adhesive tape test, an adhesion test by using the scratch method was also carried out, through which it was observed that the coating is penetrated from the first mm of the imprint length.

The highest value of the critical force (F_C) was obtained for undoped HAp (H) based coatings, with a value of 3.15 N, followed by the HAp coatings with Zn, namely H-Zn1, with

2.95 N and 2.77 N for the H-Zn2. Lower values were obtained for the Mg-doped HAp coatings, with values of 2.23 N for H-Mg1 and 1.68 N for H-Mg2.

In addition, the elemental composition after the scratch test was investigated in the center and at the end of the scratch (Figure 5.16), to identify if any calcium phosphates has remained on the surface after the penetrator had passed.
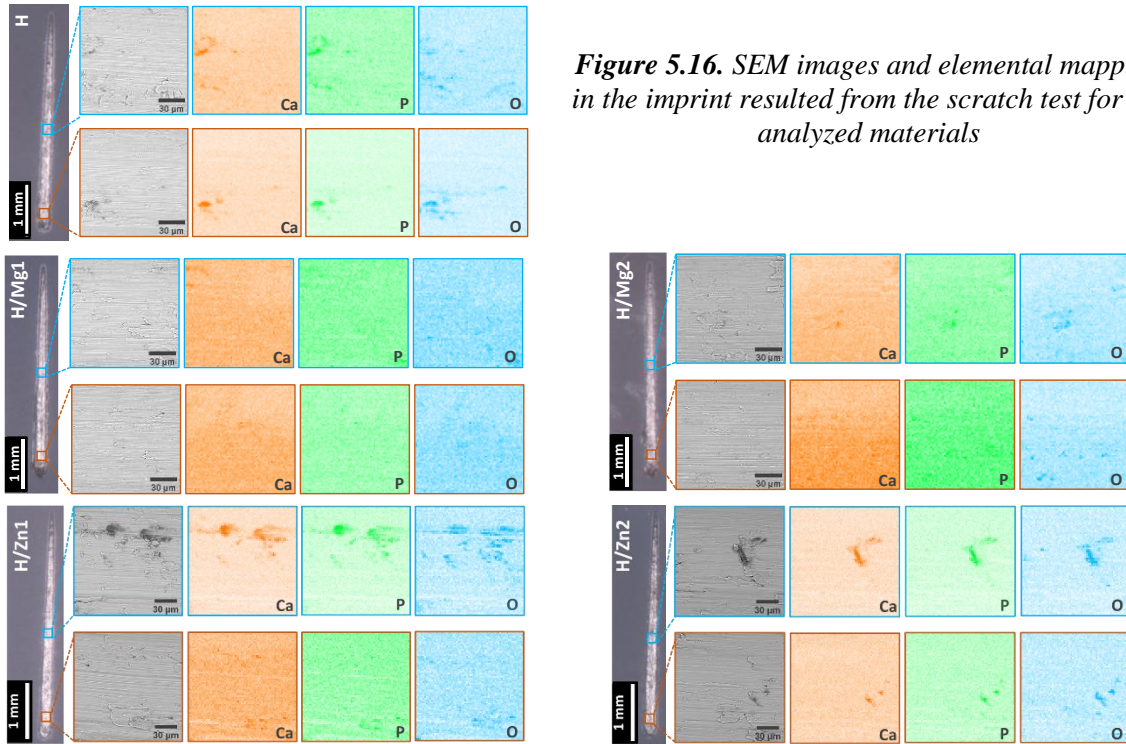
Figure 5.16. *SEM images and elemental mapping in the imprint resulted from the scratch test for the analyzed materials*

5.2.8 Surface energy

The surface energy was calculated, based on the data obtained from the contact angle investigations of the developed surfaces with the three liquids.

According to the results obtained, it can be observed that the biofunctionalization of the nanostructured surface with titanium dioxide nanotubes and with hydroxyapatite-based coatings undoped (H) and doped with Mg (H-Mg1) or Zn (H-Zn1) has led to an improvement of the surface energy from a value of 61.9 mN/m obtained for the NT surface, to a value of 64.7 mN/m for the undoped HAp (H) coatings.

The surface free energy of the polished Ti, presents values that vary between 33.5 mN/m and 49.17 mN/m [222,223], thus, comparing these values with those obtained in the present doctoral thesis, it is noted that the biofunctionalization of Ti with titanium dioxide nanotubes and subsequently coating it with HAp-based layers undoped and doped Mg or Zn leads to a substantial improvement of the wettability.

In terms of the doping elements, it is observed that their addition in the HAp structure has led to a slight improvement of the total surface free energy, reaching values of 66.9 mN/m for H-Mg1 and 65.8 mN/ m for H-Zn1. Compared to the NT surface, the H-Mg1 sample has the highest surface energy, followed by H-Zn1 and H, indicating that addition of Mg or Zn improves the surface characteristics of the HAp-based coatings.

Chapter 6. Testing the properties of the nanostructured surfaces and biofunctionalized with hydroxyapatite-based coatings

In this chapters are presented the results obtained after testing the new surfaces developed in this doctoral thesis, in terms of electrochemical behavior, bioactivity, biocompatibility, and antibacterial efficiency.

The tests were carried out on the materials selected based on the investigations performed in Chapter 5, and comprise samples of pure Ti with the surface:

- polished (Ti-L),
- nanostructured with titanium dioxide nanotubes (NT),
- nanostructured with titanium dioxide nanotubes and coated with undoped hydroxyapatite (H)
- nanostructured with titanium dioxide nanotubes and coated with hydroxyapatite doped with Mg (H-Mg) or Zn (H-Zn) obtained in electrolytes with the lower amount of the doping element.

6.1 Testing the electrochemical behavior

The electrochemical polarization tests (Tafel plots) were used to study the electrochemical behavior of the substrate (NT) and the developed HAp based coatings. The tests were carried out in two simulated biological mediums, namely: simulated body fluid (SBF) and Fusayama-Meyer artificial saliva (SA).

6.1.1 Electrochemical polarization tests

Based on the obtained results, it can be concluded that addition of Mg leads to a weaker electrochemical behavior of HAp, due to the nature of this element, namely, to be degradable, allowing so to control the degradation capacity of HAp. On the other hand, the addition of Zn in the HAp structure leads to an improvement of the electrochemical behavior, compared to Mg-doped HAp-based coatings, because Zn exhibits a lower degradation rate compared to Mg. In conclusion, it can be stated that the electrochemical properties of HAp-based coatings can be modulated by addition of Mg or Zn into the HAp structure

6.1.2 Morphological investigation of the coatings after the electrochemical tests

After performing the electrochemical tests, the investigated materials were analyzed in terms of morphology with a scanning electron microscope and no significant changes of the morphology were observed, indicating that they are stable following the interaction with the testing medium during the electrochemical tests.

6.2 Bioactivity evaluation in simulated biological mediums

The biomineralization and biodegradation tests were carried out in order to evaluate the bioactivity of the newly developed surfaces on pure Ti. The polished Ti and the nanostructured surface with titanium dioxide nanotubes weren't considered for these tests, since the kinetics of the titanium degradation/corrosion process is quite low, so that during the 21 days no obvious results can be registered in terms of mass evolution.

6.2.1 *In vitro* biomineralization tests

The biomineralization tests (apatite precipitation) were performed by immersing the samples in SBF for a predetermined period, of a maximum of 21 days.

6.2.1.1 Mass evolution

In simulated body fluid (SBF), all materials obtained by biofunctionalization of the pure Ti surface, namely, the nanostructured surface uncoated (NT) and coated with hydroxyapatite undoped (H) and doped with Mg (H-Mg) or Zn (H-Zn), have improved the biomineralization

capacity of the polished titanium (Ti-L), regardless the immersion period. Regarding the evolution of the newly formed apatite mass, except for Ti-L which had the weakest evolution, it is noted that the uncoated nanostructured surface (NT) recorded the lowest mass evolution, compared to the one coated with undoped or doped HAp, indicating that biofunctionalization with HAp-based bioactive ceramic layers, favors the precipitation of a larger amount of apatite on the surface.

6.2.1.2 Morphological and phasic composition analysis of the surfaces after the biomineralization tests

It is worth noting that in SBF, on all surfaces modified by electrochemical techniques, a layer of newly apatite was formed over the entire surface, showing a morphology composed of semi-spherical crystals, demonstrating that the developed surfaces present superior bioactive properties than pure titanium (Ti-L), as well as good biomineralization capacity in SBF. This morphology consisting of semi-spherical crystals is typical for the apatite precipitated from SBF [229,230].

According to the X-Ray diffraction results it was noted that after 21 days of immersion in SBF, the NT surface and the undoped and doped HAp-based coatings, show well defined diffraction peaks, specific for HAp according to the standard (ICDD #09-0432), confirming its presence, and thus highlighting that the obtained coatings have a bioactive character that favors osseointegration. Compared to the biofunctionalized surfaces, the Ti-L does not present the diffraction peaks specific to calcium phosphates, confirming both the weight/mass evolution and SEM analysis.

6.2.2 *In vitro* biodegradation tests

In order to estimate the biodegradability capacity of the coatings, immersion tests were carried out in phosphate buffer solution (PBS). The samples were immersed in PBS for a period of 21 days and monitored for different time intervals (1 day, 3 days, 7 days, 14 days and 21 days).

6.2.2.1 Mass evolution of the coatings

In terms of biodegradation in PBS, it was observed that addition of the doping elements has improved the degradation capacity of HAp. In conclusion, regarding the degradation capacity of the HAp-based coatings it can be stated, that addition of Mg or Zn doping elements has led to an acceleration of the degradation processes of the HAp-based layers.

6.2.2.2 Morphological and phasic composition analysis of the surfaces after the biodegradation tests

The morphology of the coatings after immersion in PBS confirms the results obtained from the mass evolution analysis, noting that towards the peaks, the ribbons show signs of degradation (H-Mg and H-Zn), as well as a reduction of the ribbons dimension, in the case of undoped HAp coatings (H).

The diffractograms obtained for the nanostructured surfaces coated with HAp-based layers undoped (H) and doped with Mg (H-Mg) or Zn (H-Zn), show a similar appearance to the ones before immersion, indicating that the obtained materials are relatively stable and that no other types of phases were formed in PBS after 21 days of immersion. However, it should be noted that, compared to the initial ones, some small differences in terms of intensities were observed.

6.3 Biocompatibility evaluation through cell viability assays

6.3.1 Morphology, proliferation and cell viability

For monitoring the colonization with osteoblast cells from the MG63 line of the pure Ti samples with a polished surface (Ti-L), the nanostructured surface with titanium dioxide

nanotubes uncoated (NT) and coated with HAp-based layers undoped (H) and doped with Mg (H-Mg) or Zn (H-Zn), fluorescence experiments were performed, allowing so the visualization of the β actin cytoskeleton (green color) and the nucleus (blue color).

The cell viability results highlighted that from cell viability point of view, the electrochemical techniques proposed for the biofunctionalization of the pure Ti surface, namely anodic oxidation and electrochemical deposition by pulsed galvanostatic method, have improved the *in vitro* behavior of pure Ti.

The cell viability results obtained for H-Mg and H-Zn coatings are in good correlation with literature data, stating that the Mg^{2+} ions from the Mg-doped HAp, favor cell adhesion and proliferation [58,236] while Zn in certain concentrations [209,214], leads to a higher cell viability, compared to undoped HAp.

Studies [56,206,236,237] indicate that in the case of HAp-Zn and H-Mg coatings, Zn^{2+} and Mg^{2+} ions are released through degradation processes, favoring so the cell proliferation. Thus, from the biodegradation tests (§6.3.2) it was demonstrated that HAp-based coatings doped with Mg or Zn improve the degradation capacity of HAp.

6.4 Evaluation of the antibacterial efficiency

According to the results obtained from the antibacterial efficiency tests to *E. coli*, which were carried out on the experimental samples, the following aspects can be stated.

The positive values indicate antibacterial efficiency, thus, the nanostructured surface uncoated (NT) and coated with undoped (H) and Zn-doped (H-Zn) HAp-based coating indicates a good antibacterial character. The negative values of the antibacterial efficiency indicate a possible activation of the *E. coli* bacteria, so it was observed that the addition of Mg in the HAp structure does not induce an antibacterial effect. Such results for Mg-based HAp coatings have also been reported in other studies [239,240].

In conclusion, it can be said that the nanostructured surface uncoated and coated with Zn-doped HAp provides a good antibacterial efficiency, while the addition of Mg leads to possible activation of bacteria, showing a poor antibacterial efficiency.

Conclusions, personal contributions and future research directions

Currently, the problem of obtaining hydroxyapatite-based coatings doped with biocompatible elements, having predetermined properties of bioactivity but also antibacterial capabilities, is a very hot research topic, with broad perspectives of applicability. To the same extent, development of the surfaces modified at nanometric level, of the metallic implantable medical devices, which can support the growth and adhesion of new tissue, can also be mentioned. A proper selection of the coating type or surface, in agreement with to the implantation site, and the role that it has to accomplish, can lead to a successful implantation of the medical devices.

General conclusions

The doctoral thesis " *Studies and research on improving the osseointegration properties of titanium through electrochemical techniques*" represents a complex study that addresses a current problem in medicine, namely the improvement of the osseointegration capacity of Ti-based metallic biomaterials, and offers, as an original solution, the usage of electrochemical methods for the biofunctionalization of the Ti surface with a nanostructured surface with titanium dioxide nanotubes obtained through anodic oxidation, which will be further coated with a layer of hydroxyapatite bioactive ceramic undoped, and doped with biocompatible elements, such as Mg and Zn. The coatings were obtained by electrochemical deposition using the pulsed galvanostatic technique

Thus, the following conclusions could be stated:

Preliminary experimental results

1. Nanostructured surfaces with titanium dioxide nanotubes with a diameter of approx. 70 nm, optimal for favorable osseoconductivity and osseointegration, with a strong hydrophilic character and good anticorrosive properties, were obtained through anodic oxidation technique;

2. An optimal crystallization treatment of the nanostructured surfaces was carried out, which has led to the transformation of the titanium dioxide developed on the titanium surface in the form of nanotubes, from an amorphous state to a crystalline one;

3. Mg-doped hydroxyapatite coatings with different concentrations of the doping element, were obtained through the galvanostatic electrochemical technique in pulses, in order to identify the effects on the properties of the hydroxyapatite, with the aim of selecting them for a subsequent deposition on a titanium substrate with a nanostructured surface with titanium dioxide nanotubes;

Experimental results

4. The use of the galvanostatic electrochemical deposition technique in pulses has led to development of HAp coatings undoped and doped with Mg or Zn, on the surface of nanostructured titanium with titanium dioxide nanotubes, with a uniform and compact aspect, covering the entire surface exposed to the electrolyte;

5. All coatings obtained show a single type of ***morphology***, namely, ribbon-like; the Mg-doped HAp layers show small changes in terms of morphology, compared to undoped HAp, which consist of a slight increase of the ribbons dimension, being a little wider, when the coatings are obtained in an electrolyte that contains a concentration of 1 mM $Mg(NO_3)_2$;

6. Compared to undoped and Mg-doped HAp, and regardless of the Mg concentration, the Zn-doped HAp coatings show much smaller ribbon dimensions in terms of width, which decrease by increasing the Zn concentration;

7. In terms of the ***formation mechanism*** of the HAp-based coatings obtained by galvanostatic deposition in pulses, it was highlighted that the obtained coatings are made of (in section) of two layers with different morphologies; the first layer, is formed in the first part of the electrochemical deposition process, and consists of plate-like crystals, with a more compact appearance and a lower thickness, compared to the second layer, which has a higher thickness, and which consists of long and thin ribbon-like crystals grown perpendicular on the substrate;

8. According to the ***elemental composition*** results, the (Ca+M)/P ratio decreases with the addition of doping elements; all coatings show a smaller (Ca+M)/P ratio than that of stoichiometric HAp of 1.67, suggesting that the doping process leads to the formation of Ca-deficient HAp;

9. Regarding the ***phasic composition***, it can be said that hydroxyapatite is the main phase in all the coatings developed, identifying also a secondary phase, namely monetite which is a precursor of HAp; other diffraction peaks identified in all coatings were attributed to both pure Ti and titanium dioxide, through its two phases, namely, anatase and rutile; no diffraction peaks specific to the doping elements in their metallic form were identified;

10. All diffractograms show the same allure and diffraction peaks, with small differences in terms of intensities, irrespective of the doping element used (Mg or Zn), as well as their concentration;

11. The diffraction peaks of HAp from ~ 26° associated to the (002) plane, changes its intensity and shifts slightly to the right, indicating that the Mg and Zn ions are replacing the Ca ones from the HAp structure, demonstrating the doping/substitution effect;

12. Regarding the calculated *structural parameters*, it can be stated that they decrease with the addition of the doping elements, indicating the deformation of the HAp crystal lattice and confirming the substitution of the Ca ions with those of the doping element;

13. An increase in the crystallite size is observed after the addition of Mg or Zn into the HAp, regardless the dopant concentration;

14. Irrespective of the doping element type, the *crystallinity degree* of HAp has increased after their addition; it has increased by increasing the Mg concentration, and has decreased by increasing the Zn concentration;

15. The **chemical bonds** investigations have revealed the present of the phosphate group (PO_4^{3-}) and hydroxyl groups (OH-) in all coatings, the most intense being noted in the case of the undoped HAp-based coatings; the presence of PO_4^{3-} group between 900 and 1100 cm^{-1} confirms the formation of HAp phase; addition of Mg or Zn, has led to a decrement in its intensity with respect to the doping element concentration, so, the higher the amount of the doping element, the weaker the intensity became, indicating the loss of the OH- groups from the unit cell and the substitution with Zn or Mg ions;

16. All coatings present a **roughness** higher than the one obtained for the polished titanium and the one nanostructured with titanium dioxide nanotubes; the roughness of the HAp coatings increases with the addition of Mg in its structure and decreases when the Mg concentration increases; the roughness of the Zn-doped HAp coatings shows a smaller roughness than that of the undoped HAp, and by increasing the Zn concentration a decrease of the roughness is observed;

17. The **thicknesses** of the developed HAp coatings presents values between 5.5 and 13.7 µm, the highest value was noted for the HAp coating doped with Mg which was obtained in the electrolyte with a concentration of 1.5 mM of Mg(NO₃)₂, while the smallest value was noted for the HAp coatings doped with Zn obtained in the electrolyte with a concentration of 0.02 mM of Zn(NO₃)₂; increasing the Mg concentration leads to a increment of the coating thickness, while by increasing the amount of Zn leads to its decrement;

18. Following the **adhesion tests** carried out by adhesive tape test, it can be said that all coatings had a good adhesion to the surface of the titanium nanostructured with titanium dioxide nanotubes, with better results being registered for the HAp based coatings undoped and doped with Mg or Zn obtained in the electrolytes with a lower concentration of the doping element; by increasing the concentration of the doping element, the adhesion decreases causing the coatings to be classified in a lower category;

19. The critical forces registered for the doped HAp coatings during the adhesion tests by using the scratch method, are smaller than the ones obtained for the undoped HAp coatings, suggesting that addition of Mg or Zn ions in the HAp structure leads to decrement of the adhesion; by increasing the concentration of the doping element, regardless of its nature, also leads to a decrease of the critical force;

20. The results of the adhesion tests by scratch method have led to an evaluation of the coatings adhesion in a similar way to the ones obtained from the adhesive tape method;

21. Within the imprint/scratch resulted after performing the scratch adhesion tests, the presence of Ca and P traces was demonstrated, being a beneficial fact in case the coatings are damaged during implantation due to their friction with the hard tissue, or a due to a possible careless handling of the medical devices coated with HAp;

22. The nanostructured surface uncoated and coated with HAp based coatings undoped or doped with Mg or Zn show a strong hydrophilic character, irrespective of the liquid used to perform the **contact angle** measurement;

23. The **surface free energy** has registered higher values after the nanostructured surface was coated with HAp based layers undoped or doped with Mg or Zn; compared to the undoped HAp, the doping elements have led to an enhancement (increment) of the surface energy;

24. By nanostructuring the titanium surface with titanium dioxide nanotubes, the **corrosion resistance** in both SBF and SA medium, has increased;

25. Deposition of undoped HAp layers on the nanostructured surface with titanium dioxide nanotubes improves its ***electrochemical behavior*** in both testing mediums (SBF and SA); addition of Mg into HAp has led to a weaker electrochemical behavior and a possible more pronounced degradation of the deposited coatings; addition of Zn ions into HAp has induced a weaker electrochemical behavior of this coatings compared to undoped HAp one, but better than that of Mg-doped HAp;

26. The electrochemical techniques used for surface biofunctionalization have improved the Ti ***biomineralization capacity*** in SBF, regardless the immersion period; the highest amount of newly formed apatite at the end of the biomineralization tests was registered for the Zn-doped HAp coatings, followed by Mg-doped HAp ones, demonstrating so, an enhancement of the bioactivity of these materials in terms of biomineralization capacity;

27. During the ***biodegradation*** tests, the HAp coatings doped with Mg have registered the highest mass loss at the end of the 21 days of immersion in PBS, demonstrating that addition of this element, leads to an acceleration of the degradation processes of HAp;

28. The ***cell viability*** tests with osteoblast cell cultures demonstrated that the electrochemical techniques (anodic oxidation and pulsed galvanostatic deposition) used for the biofunctionalization of titanium have improved the *in vitro* behavior of the newly developed surfaces; at the end of the 3-day cell viability test, the Mg-doped HAp coatings showed the highest cell viability, followed by the Zn-doped HAp coatings;

29. The highest ***antibacterial efficiency***, following the tests on *E. Coli* bacteria cultures, was recorded in the case of Zn-doped HAp coatings with a value of 16.25% compared to the control sample.

Personal contributions

The novelty of this doctoral thesis derives from the very selection of biofunctionalization methods, that can later be easily implemented for surface modification of the implantable medical devices with complex geometries, manufactured from titanium (e.g.: dental implant).

The personal contributions resulted from this research, can be summarized as follows:

- Performing a literature overview, focused on the electrochemical techniques used for the functionalization the titanium surface in order to enhance the interaction with the living tissues (biofunctionalization), and that of the biomaterials used in dental medicine for dental implants manufacturing, with a special attention directed towards titanium and its alloys, and also on hydroxyapatite;

- Identification and selection of the methods for nanostructuring the titanium surface with titanium dioxide nanotubes, and subsequently to coat this surface with hydroxyapatite-based layers;

- Identification and selection of electrochemical parameters in order to obtain hydroxyapatite-based coatings undoped and doped with biocompatible elements through electrochemical means, by using the galvanostatic method in pulses;

- Development of hydroxyapatite-based coatings undoped and doped with different concentrations of magnesium or zinc on the nanostructured surface, by using the same electrochemical deposition parameters (the electrolyte temperature during the deposition process, the applied current density, the electrolyte's pH, the number and duration of the applied pulses);

- Selection of the hydroxyapatite doping elements with the aim to obtain biocompatible, bioactive, biodegradable and/or antibacterial coatings;

- Development of zinc-doped hydroxyapatite-based coatings on a nanostructured surface with titanium dioxide nanotubes through pulsed galvanostatic electrochemical technique, which is a worldwide novelty;

- Development of hydroxyapatite-based coatings doped with zinc in optimum concentration, which can provide a good antibacterial effect, favoring at the same time the cell proliferation, without inducing a cytotoxic effect;
- A comparative, complex and detailed characterization of the nanostructured surfaces with titanium dioxide nanotubes uncoated and coated with hydroxyapatite-based coatings undoped and doped with magnesium or zinc in different concentrations, through modern investigation and characterization methods, and techniques such as scanning electron microscopy (SEM and HR-SEM), energy dispersive X-ray spectrometry (EDS), incident angle X-ray diffraction (GI-XRD), Fourier transform infrared spectrometry (FTIR). Also, the adhesion of the coating to the nanostructured surface with titanium dioxide nanotubes was carried out by the adhesive tape test and the scratch test;
- Complex testing of the nanostructured surfaces with titanium dioxide nanotubes uncoated and coated with hydroxyapatite-based coatings undoped and doped with magnesium or zinc in the selected concentrations, that consisted in:
  - evaluation of the electrochemical behavior in simulated biological mediums (synthetic body fluid - SBF and artificial saliva - SA);
  - evaluation of the bioactivity through biomineralization tests in SBF and biodegradation in phosphate buffer solution (PBS);
  - evaluation of the biocompatibility through cell viability tests with MG63 osteoblast cells;
  - evaluation of the antibacterial efficiency by using *E. coli* bacterial cell cultures.

Future research directions

Some issues addressed in this study remains open for a further, more extensive and, if necessary, thorough approach. This category includes the following:
- Quantification and identification of the ions released in the solutions, following the bioactivity and the electrochemical behavior tests;
- Evaluation at a micro- and nanometric level of the titanium-nanotubes and nanotubes-hydroxyapatite interfaces, in order to extend the knowledge regarding the interaction and the adhesion between these materials;
- The identification or development of an adhesion testing method with a higher degree of accuracy for the materials developed in the present doctoral thesis;
- The usage of the electrochemical techniques developed in this doctoral thesis in order to biofunctionalize the surface of an implantable medical device with a complex geometry;
- Extending the period of the cell viability testing with osteoblast cell cultures, in order to highlight the biological performances on the long-term;
- Advanced studies regarding the biocompatibility of the developed materials, by performing other types of tests (cytotoxic potential, proliferation, apoptosis);
- Carrying out *in vivo* tests on animal models, of the developed materials, in order to establish the degree of toxicity and the adverse reactions upon contact with living tissues.

Selective bibliography

[4] D.F. Williams, The Williams Dictionary of Biomaterials, Liverpool University Press, 1999. https://doi.org/10.5949/UPO9781846314438.

[5] M. Niinomi, Metallic biomaterials, Journal of Artificial Organs. 11 (2008) 105–110. https://doi.org/10.1007/s10047-008-0422-7.

[7] M.S. Safavi, F.C. Walsh, M.A. Surmeneva, R.A. Surmenev, J. Khalil-Allafi, Electrodeposited Hydroxyapatite-Based Biocoatings: Recent Progress and Future Challenges, Coatings. 11 (2021) 110. https://doi.org/10.3390/coatings11010110.

[46] A. Vladescu, D.M. Vranceanu, S. Kulesza, A.N. Ivanov, M. Bramowicz, A.S. Fedonnikov, M. Braic, I.A. Norkin, A. Koptyug, M.O. Kurtukova, M. Dinu, I. Pana, M.A. Surmeneva, R.A. Surmenev, C.M. Cotrut, Influence of the electrolyte's pH on the properties of electrochemically deposited hydroxyapatite coating on additively manufactured Ti64 alloy, Sci Rep. 7 (2017). https://doi.org/10.1038/s41598-017-16985-z.

[48] D.M. Vranceanu, E. Ungureanu, *I.C. Ionescu*, A.C. Parau, A.E. Kiss, A. Vladescu, C.M. Cotrut, Electrochemical Surface Biofunctionalization of Titanium through Growth of TiO2 Nanotubes and Deposition of Zn Doped Hydroxyapatite, Coatings. 12 (2022) 69. https://doi.org/10.3390/coatings12010069.

[49] C.M. Cotrut, E. Ungureanu, *I.C. Ionescu*, R.I. Zamfir, A.E. Kiss, A.C. Parau, A. Vladescu, D.M. Vranceanu, A. Saceleanu, Influence of Magnesium Content on the Physico-Chemical Properties of Hydroxyapatite Electrochemically Deposited on a Nanostructured Titanium Surface, Coatings. 12 (2022) 1097. https://doi.org/10.3390/coatings12081097.

[58] I.M. Chirică, A.-M. Enciu, T. Tite, M. Dudău, L. Albulescu, S.L. Iconaru, D. Predoi, I. Pasuk, M. Enculescu, C. Radu, C.G. Mihalcea, A.-C. Popa, N. Rusu, S. Niţă, C. Tănase, G.E. Stan, The Physico-Chemical Properties and Exploratory Real-Time Cell Analysis of Hydroxyapatite Nanopowders Substituted with Ce, Mg, Sr, and Zn (0.5–5 at.%), Materials. 14 (2021) 3808. https://doi.org/10.3390/ma14143808.

[75] S. Lerouge, Sterilization and cleaning of metallic biomaterials, in: Metals for Biomedical Devices, Elsevier, 2019: pp. 405–428. https://doi.org/10.1016/B978-0-08-102666-3.00016-X.

[82] K. von der Mark, J. Park, Engineering biocompatible implant surfaces. Part II: Cellular recognition of biomaterial surfaces: Lessons from cell-matrix interactions, Prog Mater Sci. 58 (2012) 327–381. https://doi.org/10.1016/j.pmatsci.2012.09.002.

[83] J.G. Caton, G. Armitage, T. Berglundh, I.L.C. Chapple, S. Jepsen, K.S. Kornman, B.L. Mealey, P.N. Papapanou, M. Sanz, M.S. Tonetti, A new classification scheme for periodontal and peri-implant diseases and conditions - Introduction and key changes from the 1999 classification, J Clin Periodontol. 45 (2018) S1–S8. https://doi.org/10.1111/jcpe.12935.

[85] M.M.M. Abir, Y. Otsuka, K. Ohnuma, Y. Miyashita, Effects of composition of hydroxyapatite/gray titania coating fabricated by suspension plasma spraying on mechanical and antibacterial properties, J Mech Behav Biomed Mater. 125 (2022) 104888. https://doi.org/10.1016/j.jmbbm.2021.104888.

[94] K. Indira, U.K. Mudali, T. Nishimura, N. Rajendran, A Review on TiO2 Nanotubes: Influence of Anodization Parameters, Formation Mechanism, Properties, Corrosion Behavior, and Biomedical Applications, J Bio Tribocorros. 1 (2015) 28. https://doi.org/10.1007/s40735-015-0024-x.

[100] T. Traini, G. Murmura, B. Sinjari, G. Perfetti, A. Scarano, C. D'Arcangelo, S. Caputi, The Surface Anodization of Titanium Dental Implants Improves Blood Clot Formation Followed by Osseointegration, Coatings. 8 (2018) 252. https://doi.org/10.3390/coatings8070252.

[102] C.M. Cotrut, *I.C. Ionescu*, E. Ungureanu, A. Berbecaru, R.I. Zamfir, A. Vladescu, D.M. Vranceanu, Evaluation of surface modification techniques on the ability of apatite formation and corrosion behavior in synthetic body fluid: An in vitro study, Surfaces and Interfaces. 22 (2021) 100866. https://doi.org/10.1016/j.surfin.2020.100866.

[120] Y. Sul, The significance of the surface properties of oxidized titanium to the bone response: special emphasis on potential biochemical bonding of oxidized titanium implant, Biomaterials. 24 (2003) 3893–3907. https://doi.org/10.1016/S0142-9612(03)00261-8.

[123] N. Wang, H. Li, W. Lü, J. Li, J. Wang, Z. Zhang, Y. Liu, Effects of TiO2 nanotubes with different diameters on gene expression and osseointegration of implants in minipigs, Biomaterials. 32 (2011) 6900–6911. https://doi.org/10.1016/j.biomaterials.2011.06.023.

[136] D.S. Jayakrishnan, Electrodeposition: the versatile technique for nanomaterials, Woodhead Publishing Limited, 2012. https://doi.org/10.1533/9780857095800.1.86.

[137] R. Drevet, H. Benhayoune, Electrodeposition of Calcium Phosphate Coatings on Metallic Substrates for Bone Implant Applications: A Review, Coatings. 12 (2022) 539. https://doi.org/10.3390/coatings12040539.

[141] D.M. Vranceanu, *I.C. Ionescu*, E. Ungureanu, M.O. Cojocaru, A. Vladescu, C.M. Cotrut, Magnesium doped hydroxyapatite-based coatings obtained by pulsed galvanostatic electrochemical deposition with adjustable electrochemical behavior, Coatings. 10 (2020) 1–15. https://doi.org/10.3390/COATINGS10080727.

[142] D. Gopi, J. Indira, L. Kavitha, A comparative study on the direct and pulsed current electrodeposition of hydroxyapatite coatings on surgical grade stainless steel, Surf Coat Technol. 206 (2012) 2859–2869. https://doi.org/10.1016/j.surfcoat.2011.12.011.

[147] T. Kokubo, H. Takadama, How useful is SBF in predicting in vivo bone bioactivity?, Biomaterials. 27 (2006) 2907–2915. https://doi.org/10.1016/j.biomaterials.2006.01.017.

[158] F. Mansfeld, The Polarization Resistance Technique for Measuring Corrosion Currents, in: M.G. Fontana, R.W. Staehle (Eds.), Advances in Corrosion Science and Technology, Volume 6, Springer US, Boston, MA, 1976: pp. 163–262. https://doi.org/10.1007/978-1-4684-8986-6_3

[170] E.P. Su, D.F. Justin, C.R. Pratt, V.K. Sarin, V.S. Nguyen, S. Oh, S. Jin, Effects of titanium nanotubes on the osseointegration, cell differentiation, mineralisation and antibacterial properties of orthopaedic implant surfaces, Bone Joint J. 100-B (2018) 9–16. https://doi.org/10.1302/0301-620X.100B1.BJJ-2017-0551.R1.

[171] L. Bai, Y. Zhao, P. Chen, X. Zhang, X. Huang, Z. Du, R. Crawford, X. Yao, B. Tang, R. Hang, Y. Xiao, Targeting Early Healing Phase with Titania Nanotube Arrays on Tunable Diameters to Accelerate Bone Regeneration and Osseointegration, Small. 17 (2021) 2006287. https://doi.org/10.1002/smll.202006287.

[185] S. Ferraris, S. Spriano, G. Pan, A. Venturello, C.L. Bianchi, R. Chiesa, M.G. Faga, G. Maina, E. Vernè, Surface modification of Ti–6Al–4V alloy for biomineralization and specific biological response: Part I, inorganic modification, J Mater Sci Mater Med. 22 (2011) 533–545. https://doi.org/10.1007/s10856-011-4246-2.

[186] R. Baboian, J.R. Scully, S.W.J. Dean, Corrosion Tests and Standards, Volume 6, Springer US Plenum Press, New York, 2005.

[190] H. Wang, N. Eliaz, Z. Xiang, H.P. Hsu, M. Spector, L.W. Hobbs, Early bone apposition in vivo on plasma-sprayed and electrochemically deposited hydroxyapatite coatings on titanium alloy, Biomaterials. 27 (2006) 4192–4203. https://doi.org/10.1016/j.biomaterials.2006.03.034.

[191] K. Kanamoto, K. Imamura, N. Kataoka, J. Oshitani, H. Imanaka, K. Nakanishi, Formation characteristics of calcium phosphate deposits on a metal surface by H2O2-electrolysis reaction under various conditions, Colloids Surf A Physicochem Eng Asp. 350 (2009) 79–86. https://doi.org/10.1016/j.colsurfa.2009.09.007.

[195] B. Bakin, T. Koc Delice, U. Tiric, I. Birlik, F. Ak Azem, Bioactivity and corrosion properties of magnesium-substituted CaP coatings produced via electrochemical deposition, Surf Coat Technol. 301 (2016) 29–35. https://doi.org/10.1016/j.surfcoat.2015.12.078.

[196] L. Morejón-Alonso, C. Mochales, L. Nascimento, W. Müller, Electrochemical deposition of Sr and Sr/Mg-co-substituted hydroxyapatite on Ti-40Nb alloy, Mater Lett. 248 (2019) 65–68. https://doi.org/10.1016/j.matlet.2019.03.141.

[204] I. Uysal, F. Severcan, A. Tezcaner, Z. Evis, Co-doping of hydroxyapatite with zinc and fluoride improves mechanical and biological properties of hydroxyapatite, Progress in Natural Science: Materials International. 24 (2014) 340–349. https://doi.org/10.1016/j.pnsc.2014.06.004.

[205] N. v. Bulina, O.B. Vinokurova, N. v. Eremina, I.Y. Prosanov, V.R. Khusnutdinov, M. v. Chaikina, Features of solid-phase mechanochemical synthesis of hydroxyapatite doped by copper and zinc ions, J Solid State Chem. 296 (2021) 121973. https://doi.org/10.1016/j.jssc.2021.121973.

[206] Y. Yajing, D. Qiongqiong, H. Yong, S. Han, X. Pang, Magnesium substituted hydroxyapatite coating on titanium with nanotublar TiO2 intermediate layer via electrochemical deposition, Appl Surf Sci. 305 (2014) 77–85. https://doi.org/10.1016/j.apsusc.2014.02.163.

[209] Q. Ding, X. Zhang, Y. Huang, Y. Yan, X. Pang, In vitro cytocompatibility and corrosion resistance of zinc-doped hydroxyapatite coatings on a titanium substrate, J Mater Sci. 50 (2015) 189–202. https://doi.org/10.1007/s10853-014-8578-4.

[210] Y. Cai, S. Zhang, X. Zeng, Y. Wang, M. Qian, W. Weng, Improvement of bioactivity with magnesium and fluorine ions incorporated hydroxyapatite coatings via sol–gel deposition on Ti6Al4V alloys, Thin Solid Films. 517 (2009) 5347–5351. https://doi.org/10.1016/j.tsf.2009.03.071.

[214] A. Ito, K. Ojima, H. Naito, N. Ichinose, T. Tateishi, Preparation, solubility, and cytocompatibility of zinc-releasing calcium phosphate ceramics, J Biomed Mater Res. 50 (2000) 178–183. https://doi.org/10.1002/(SICI)1097-4636(200005)50:2<178::AID-JBM12>3.0.CO;2-5.

[220] R. Narayanan, S.K. Seshadri, T.Y. Kwon, K.H. Kim, Review Calcium Phosphate-Based Coatings on Titanium and Its Alloys, (2007) 279–299. https://doi.org/10.1002/jbm.b.30932.

[222] R.M. do Nascimento, V.R. de Carvalho, J.S. Govone, A.C. Hernandes, N.C. da Cruz, Effects of negatively and positively charged Ti metal surfaces on ceramic coating adhesion and cell response, J Mater Sci Mater Med. 28 (2017) 33. https://doi.org/10.1007/s10856-017-5848-0.

[223] L. Ponsonnet, K. Reybier, N. Jaffrezic, V. Comte, C. Lagneau, M. Lissac, C. Martelet, Relationship between surface properties (roughness, wettability) of titanium and titanium alloys and cell behaviour, Materials Science and Engineering C. 23 (2003) 551–560. https://doi.org/10.1016/S0928-4931(03)00033-X.

[229] T. Kokubo, Design of bioactive bone substitutes based on biomineralization process, Materials Science and Engineering: C. 25 (2005) 97–104. https://doi.org/10.1016/j.msec.2005.01.002.

[230] T. Kokubo, S. Yamaguchi, Novel bioactive materials developed by simulated body fluid evaluation: Surface-modified Ti metal and its alloys, Acta Biomater. 44 (2016) 16–30. https://doi.org/10.1016/j.actbio.2016.08.013.

[236] S. Chen, Y. Shi, X. Zhang, J. Ma, Biomimetic synthesis of Mg-substituted hydroxyapatite nanocomposites and three-dimensional printing of composite scaffolds for bone regeneration, J Biomed Mater Res A. 107 (2019) 2512–2521. https://doi.org/10.1002/jbm.a.36757.

[237] S. Horiuchi, M. Hiasa, A. Yasue, K. Sekine, K. Hamada, K. Asaoka, E. Tanaka, Fabrications of zinc-releasing biocement combining zinc calcium phosphate to calcium phosphate cement, J Mech Behav Biomed Mater. 29 (2014) 151–160. https://doi.org/10.1016/j.jmbbm.2013.09.005.

[239] P. Shahmohammadi, B.A. Khazaei, Characterization of Zn/Mg-enriched calcium phosphate coating produced by the two-step pulsed electrodeposition method on titanium substrate, Surfaces and Interfaces. 22 (2021) 100819. https://doi.org/10.1016/j.surfin.2020.100819.

[240] D. Franco, G. Calabrese, S. Petralia, G. Neri, C. Corsaro, L. Forte, S. Squarzoni, S. Guglielmino, F. Traina, E. Fazio, S. Conoci, Antimicrobial Effect and Cytotoxic Evaluation of Mg-Doped Hydroxyapatite Functionalized with Au-Nano Rods, Molecules. 26 (2021) 1099. https://doi.org/10.3390/molecules26041099.

List of scientific papers published

The results obtained during the doctoral thesis program were disseminated by publishing **5 articles in ISI journals**, as well as by participating at **12 international conferences**.

Scientific papers published in ranked/indexed ISI journals

1. Cotrut C.M., Ungureanu E., **Ionescu Ionut Cornel***, Zamfir R.I., Kiss A.E., Parau A.C., Vladescu A., Vranceanu M.D., Saceleanu A., *Influence of Magnesium Content on the Physico-Chemical Properties of Hydroxyapatite Electrochemically Deposited on a Nanostructured Titanium Surface*, Coatings, 2022, Vol. 12., Iss. 8., Article No. 1097, DOI: 10.3390/coatings12081097;

2. Vrânceanu, D.M., Ungureanu, E., **Ionescu Ionut Cornel**, Pârâu A.C., Kiss A.E., Vlădescu, A., Cotruț, C.M., *Electrochemical surface biofunctionalization of titanium through growth of TiO$_2$ nanotubes and deposition of Zn doped hydroxyapatite*, Coatings, 2022, Vol. 12, Iss. 1, Article No. 69, DOI: 10.3390/coatings12010069;

3. Cotruț C.M., **Ionescu Ionut Cornel**, Ungureanu E., Berbecaru A., Zamfir R.I., Vlădescu A., Vrânceanu D.M., *Evaluation of surface modification techniques on the ability of apatite formation and corrosion behavior in synthetic body fluid: An in vitro study,* Surfaces and Interfaces, 2021, Vol. 22, Article No. 100866. DOI: 10.1016/j.surfin.2020.100866;

4. Vrânceanu D.M., **Ionescu Ionut Cornel**, Ungureanu E., Cojocaru M.O., Vlădescu A., Cotruț C.M.*, *Magnesium doped hydroxyapatite obtained by pulsed galvanostatic deposition with adjustable electrochemical behavior,* Coatings, 2020, Vol. 10, Iss. 8, Article No. 727, DOI: 10.3390/coatings10080727;

5. Ungureanu E., **Ionescu Ionut Cornel**, Zamfir-Andronic R.I., Vasilescu M, Milea C.G., Dobrescu M.C., Vrânceanu D.M., Cotruț C.M., *Biofunctionalization of Ti6Al4V surface with Ag modified HAp coatings via electrochemical deposition,* UPB Scientific Bulletin, Series B: Chemistry and Materials Science, 2020, Vol. 82, Iss. 4, pp. 307-324.

Papers presented at international conferences

1. D.M. Vranceanu, **Ionescu Ionut Cornel**, E. Ungureanu, A. Kiss, A.C. Parau, C.M. Cotrut, *Influence of Mg and Zn content on the properties of hydroxyapatite based coatings,* 6th International Conference New Trends on Sensing - Monitoring - Telediagnosis for Life Sciences NT-SMT-LS 2022, September 8 - 10, 2022, Brasov, Romania (on site and online participation) - **poster**;

2. D.M. Vranceanu, **Ionescu Ionut Cornel**, E. Ungureanu, A.C. Parau, R.I. Zamfir I. Titorencu, M. Badea, C. Adochite, S. Costinas, M. Idomir, A. Vladescu and C.M. Cotrut, *In vitro evaluation of doped hydroxyapatite coatings electrochemically deposited on titanium nanostructured surface,* 6th International Conference New Trends on Sensing - Monitoring - Telediagnosis for Life Sciences NT-SMT-LS 2022, September 8 – 10, 2022, Brasov, Romania (on site and online participation) - **poster**;

3. D.M. Vranceanu, **Ionescu Ionut Cornel**, E. Ungureanu, A.C. Parau, A. Vladescu., C.M. Cotrut, *Biofunctionalization of titanium with titania nanotubes and doped hydroxyapatite-based coatings,* 9th International Conference "Biomaterials, Tissue Engineering & Medical Devices" BIOMMEDD'2022, July 20-22, 2022, Bucharest, Romania – **oral presentation**;

4. D.M. Vranceanu, **Ionescu Ionut Cornel**, E. Ungureanu, A. Kiss, G.A. Juravlea, R.I. Zamfir, I. Titorencu, A. Vladescu and C.M. Cotrut, *Physico-chemical properties and in vitro behavior of Zn doped HAp based coatings deposited on nanostructured surface*, EMRS – Spring Meeting Virtual Conference, May 30 –June 3, 2022, Strasbourg, France (on-line) – **poster**;

5. D.M. Vranceanu, E. Ungureanu, **Ionescu Ionut Cornel,** G.A. Juravlea, A. Kiss, A. Parau, A. Vladescu, C.M. Cotrut, *Biofuncationalization of Ti nanostructured surfaces with hydroxyapatite-based coatings intended for medical applications,* 3rd Coatings and

Interfaces Conference, Part of the Coatings and Interfaces series, November 24 – 26 , 2021 (on-line) – **poster**;

6. D.M. Vranceanu, **Ionescu Ionut Cornel,** E. Ungureanu, A. Berbecaru, G.A. Juravlea, R.I. Zamfir, A. Vladescu, C.M. Cotrut, *Assessment of different surface modification techniques on the corrosion behavior and the ability of apatite formation of titanium,* EMRS – Spring Meeting Virtual Conference, May 31 –June 1, 2021, Strasbourg, France (on-line) – **oral presentation**;

7. **Ionescu Ionut Cornel,** M. Cojocaru, E. Ungureanu, A. Berbecaru, D.M. Vranceanu, C.M. Cotrut, *Electrochemical behavior and adherence of hydroxyapatite-based coatings on nanostructured titanium surface*, 8th International Conference on Materials Science and Technologies, ROMAT2020, November 26-27, 2020, Bucharest, Romania (on-line) – **poster**;

8. D.M. Vranceanu, **Ionescu Ionut Cornel,** E. Ungureanu, A. Berbecaru, G.A. Juravlea, R.I. Zamfir, A. Vladescu, C.M. Cotrut, *Impact of surface modification techniques on the in vitro corrosion behavior and biomineralization ability of titanium*, ROMAT2020, November 26-27, 2020, Bucharest, Romania (on-line) – **oral presentation**;

9. E. Ungureanu., **Ionescu Ionut Cornel,** G.A. Juravlea, A.A. Cloşcă, A. Vladescu, C.M. Cotruţ, *Magnesium-doped hydroxyapatite coatings obtained by electrochemical deposition with enhanced features*, 8th International Conference on Materials Science and Technologies, ROMAT2020, November 26-27, 2020, Bucharest, Romania (on-line), **poster**;

10. **Ionescu Ionut Cornel,** D.M. Vranceanu, D. Tabaras, E. Ungureanu, A. Berbecaru, M. Cojocaru, A.C. Parau, A.Vladescu, C.M. Cotrut *Bioactivation through duplex treatment of titanium-based surface intended for biomedical applications,* 1st International Conference "Medical Materials Science & Engineering – BIOMAT" (1Biomat), 20 – 23 February, 2021, Predeal, Romania – **poster**;

11. **Ionescu Ionut Cornel,** D.M. Vranceanu, E. Ungureanu, A. Berbecaru, A.C. Parau, A.Vladescu, M. Cojocaru, C.M. Cotrut, *Nanostructured titanium dioxide surface biofunctionalized with nano-hydroxyapatite bioceramic based coating as tailored surface,* International Conference on Functional Nanomaterials and Nanodevices – NANOMAT 2019, 11 – 13 September, 2019, Prague, Czech Republic – **poster**;

12. **Ionescu Ionut Cornel,** D.M. Vranceanu, V.I. Negoiescu, A. Berbecaru, A.C. Parau, A Vladescu, M. Cojocaru, C.M. Cotrut, *Electrochemical techniques for tailored biomedical surface properties: anodized treatment and HAp deposition – a duplex treatment, The 43rd American Romanina Academy of Arts and Sciences Congress"* (ARA 34rd), 9 – 14 June, 2019, Thessaloniki, Greece **– poster**.